FACULTY
OF MATHEMATICS
AND PHYSICS
Charles University

MASTER THESIS

Bc. Kateřina Mladá

Emergence of irreversible dynamics by the lack-of-fit reduction

Mathematical Institute of Charles University

Supervisor of the master thesis: doc. RNDr. Michal Pavelka, Ph.D.

Study programme: Theoretical Physics

Study branch: FTFP

Prague 2023

I declare that I carried out this master thesis independently, and only with the cited sources, literature and other professional sources. It has not been used to obtain another or the same degree.

I understand that my work relates to the rights and obligations under the Act No. 121/2000 Sb., the Copyright Act, as amended, in particular the fact that the Charles University has the right to conclude a license agreement on the use of this work as a school work pursuant to Section 60 subsection 1 of the Copyright Act.

In . . . . date . . . .

Author's signature

Title: Emergence of irreversible dynamics by the lack-of-fit reduction

Author: Bc. Kateřina Mladá

Institute: Mathematical Institute of Charles University

Supervisor: doc. RNDr. Michal Pavelka, Ph.D., Mathematical Institute of Charles University

Abstract: The thesis studies theories of dimensional reduction on the example of the Kac-Zwanzig (heat bath) model. The studied methods are the Mori-Zwanzig projection formalism and the lack-of-fit reduction, both applied for two sets of resolved variables. The methods give integro-differential and ordinary differential evolution equations respectively. For the Mori-Zwanzig formalism, a limit of the number of particles going to infinity is made, which leads to an exponential memory kernel and consequently to a set of stochastic differential equations. The evolution equations of the two methods are compared using numerical simulations.

Keywords: irreversibility, dissipation, Hamiltonian evolution

Contents

Introduction

Imagine a physical system. For different physicist this image would be different – in the sixteenth century it might have been a wheel rolling down a hill, while in modern cosmology it might be something as complex as the whole universe. However, across all physics we are always talking about systems, which follow certain rules that we are trying to uncover and each system has scales on which these rules apply. There is an assumption, implicit or explicit, that by approaching a physical system, certain rules are at place on the time and space scale that we are observing – in other words, we assume that there is actually something to be observed.

Statistical physics looks at the problem of scales and transition between them: from the microscopic deterministic reversible dynamics governed by the most fundamental equations of motions, over stochastic Langevin dynamics on the nano scale, to the macroscopic irreversible but deterministic dynamics in thermodynamics. This transition requires us to decide, which variables are still relevant on larger scales and which ones are negligible. Such a choice of variables not only isn't unique, but also isn't the only decision made by the physicist. Most of the time when encountering a problem in a given system, there are also additional decision of what to neglect or even in what manner the system behaves – all these things are often being postulated, in order to gain comprehensible knowledge. Statistical physics is attempting to find more systematical techniques of approaching the problem of scale transition, which would justify these intuitive postulates. In this thesis, two such techniques will be studied and applied on the problem of the Kac-Zwanzig model.

The thesis will be organised as follows. The first chapter is an introduction to three theories: first of them being the Mori-Zwanzig projection formalism, second the GENERIC formalism and the third is Bruce Turkington's lack-of-fit reduction within the context of GENERIC. In the second chapter we apply the theory on the Kac-Zwanzig (heat bath) model. The application allows us to study specific problems, which arise throughout the calculations as well as compare the results of the theories. This comparison is done in the third and last chapter using numerical simulations.

1. Methods

The first chapter introduces methods of transition between levels of description. This theoretical introduction is not fully general in nature. Instead it focuses on formulations, which are going to be used in Chapter 2.

1.1 The Mori Zwanzig Formalism

Let us first focus on the Mori-Zwanzig formalism, which is also called the projection formalism, first studied in [1, 2], later work we will be referring to is [3, 4, 5]. It is a technique of transition between physical scales, which uses a projection operator to reduce the number of dimensions of the phase space – the original, detailed, space is split into subspace of some chosen, resolved, variables and the complement. The choice of the resolved variables is not unique. However, it can be guided by the system itself. For example, when a large separation of time scales is present, the natural choice for the resolved variables is linked to the longer time scales. The Mori-Zwanzig formalism introduced here is a method of constructing projectors onto these subspaces and finding the governing equations on these subspaces. Throughout this section, we will closely follow the introduction done in [3].

The formalism has effectively two steps, one of them being the construction of a projector $\mathcal{P}$ and the other is the use of the projector to split the evolution equations into the resolved and unresolved component. We will start with the evolution equations.

Let us consider a system of equations in the form:

$$\dot{\mathbf{z}}(t) = L\mathbf{z}(t), \tag{1.1}$$

where L is a linear operator and $\mathbf{z}$ are variables. An example of such linear operator is the canonical Poisson bracket with the Hamiltonian. This operator is used in classical systems, wherein the variables are positions and momenta. The solutions of these equations are trajectories in the phase space Ω ($\mathbf{z} \in \Omega$) and an initial condition $\mathbf{z}(0) = \mathbf{z}_0$ gives a unique solution, which corresponds to a trajectory $\varphi(\mathbf{z}_0, t)$. It is possible to describe the motion along such a trajectory using an evolution operator S^t acting on the initial condition $\mathbf{z}_0$. This operator is given by the equation:

$$\frac{\partial}{\partial t} S^t \mathbf{z}_0 = L S^t \mathbf{z}_0, \quad S^0 \mathbf{z}_0 = \mathbf{z}_0. \tag{1.2}$$

This is the evolution on the full phase space Ω. We will now move to the description on the two subspaces of Ω. One of the subspaces is created by the projection $\mathcal{P}$ and we will be calling it the resolved subspace, the other will be created by the orthogonal projection $(1 - \mathcal{P})$ and will be called the orthogonal subspace. Let us split the linear operator on the right hand side:

$$L = \mathcal{P}L + (1 - \mathcal{P})L,$$

where the orthogonal part $(1 - \mathcal{P})L$ can define the orthogonal evolution $S^t_\perp$ [3, 4, 6]:

$$\frac{\partial}{\partial t}S_\perp^t g = (1-\mathcal{P})LS_\perp^t g, \qquad S_\perp^0 g = S^0 g = g. \tag{1.3}$$

With this definition, the operator $S_\perp^t$ keeps functions g from the orthogonal space within this space, throughout the whole evolution[1]. Therefore, any evolution within the orthogonal space is by definition (1.3) governed solely through $S_\perp^t$. The full evolution on the other hand has both terms, which move only within the resolved subspace as well as terms, which seep away to the orthogonal subspace. This can be formalised using the Dyson formula for the operators S^t and $S_\perp^t$ [3]:

$$S^t f = S_\perp^t + \int_0^t S^{t-s}\mathcal{P}LS_\perp^s \mathrm{d}sf. \tag{1.4}$$

The Dyson formula holds at time t=0, where both evolution operators act as unity (1.3) and by using the evolution equation (1.2) and the definition of the orthogonal operator (1.3) we may show that it propagates through time:

$$LS^t f = \frac{\partial}{\partial t}S^t f = \frac{\partial}{\partial t}\left(S_\perp^t f + \int_0^t S^{t-s}\mathcal{P}LS_\perp^s f \mathrm{d}s\right) = (1-\mathcal{P})LS_\perp^t f + \mathcal{P}LS_\perp^t f +$$

$$+ \int_0^t \frac{\partial}{\partial t}S^{t-s}\mathcal{P}LS_\perp^s f \mathrm{d}s = L\left[S_\perp^t + \int_0^t S^{t-s}\mathcal{P}LS_\perp^s \mathrm{d}s\right]f$$

and thus holds for any given time $t \geq 0$. The evolution operator S^t has the linear operator L as a semigroup generator (from the defining equation (1.2)) and as a consequence $S^t L = LS^t$. Using this property we can write:

$$LS^t f = S^t L f = S^t \mathcal{P}Lf + S^t(1-\mathcal{P})Lf = S^t \mathcal{P}Lf + S^t F \ ,$$

where $F = (1-\mathcal{P})Lf$. Combining this adjustment with Equation (1.4), we finally arrive at the main evolution equation of the Mori-Zwanzig formalism:

$$\frac{\partial}{\partial t}S^t f = S^t \mathcal{P}Lf + \int_0^t S^{t-s}\mathcal{P}LS_\perp^s F \mathrm{d}s + S_\perp^t F. \tag{1.5}$$

First term is the projected evolution, second term represents the memory of the system and the last term is the noise from the degrees of freedom we lost through the projection or in other words a random force.

Let us now focus on the projectors. As was said above, the projector is chosen based on what are the relevant degrees of freedom. In Chapter 2 we study the Kac-Zwanzig model, which is a model with N small particles and additional distinguished particle in a potential field. We start on the phase space of these $N+1$ particles, described by their positions $\mathbf{Q}, \mathbf{q}_i$ and momenta $\mathbf{P}, \mathbf{p}_i$. There is several choices of projection operators. Since we will be working with particles in a

---

[1]Let $g = (1-\mathcal{P})g$, then $\frac{\partial}{\partial t}\left((1-\mathcal{P})S_\perp^t g\right) = (1-\mathcal{P})\frac{\partial}{\partial t}S_\perp^t g = (1-\mathcal{P})(1-\mathcal{P})LS_\perp^t g = (1-\mathcal{P})LS_\perp^t g = \frac{\partial}{\partial t}S_\perp^t g$ and so $S_\perp^t g = (1-\mathcal{P})S_\perp^t g$, i.e. g is orthogonal throughout the whole evolution.

temperature reservoir with a constant temperatur T, the small particles will have initial conditions pulled from the canonical probability distribution $\rho = \frac{1}{Z}e^{-\beta H}$ with H being the microscopic hamiltonian. This means that when we decide on the resolved degrees $\mathbf{Q}, \mathbf{P}$ the other particles are from this probability distribution and the projection operator has the form [3]:

$$\mathcal{P}f = \frac{\int f e^{-\beta H}\mathrm{d}[\mathbf{q}_j]\mathrm{d}[\mathbf{p}_i]}{\int e^{-\beta H}\mathrm{d}[\mathbf{q}_i]\mathrm{d}[\mathbf{p}_i]}. \tag{1.6}$$

Our second choice of resolved variables will be $(\mathbf{Q}, \mathbf{P}, \mathbf{s})$, with the variable $\mathbf{s}$ defined as $\mathbf{s} = \frac{1}{N}\sum_j(\mathbf{q}_j - \mathbf{Q})$. This is analogous to the case of the microcanonical ensemble [3, 1] with the difference that instead of the surface of constant energy we will work with the surface given by $\delta\left(\frac{1}{N}\sum_j(\mathbf{q}_j - \mathbf{Q}) - \mathbf{s}\right)$. Consequently, the conditional projector is of the form:

$$\mathcal{P}f = \frac{\int f e^{-\beta H}\delta\left(\frac{1}{N}\sum_j(\mathbf{q}_j - \mathbf{Q}) - \mathbf{s}\right)\mathrm{d}[\mathbf{q}_j]\mathrm{d}[\mathbf{p}_i]}{\int e^{-\beta H}\delta\left(\frac{1}{N}\sum_j(\mathbf{q}_j - \mathbf{Q}) - \mathbf{s}\right)\mathrm{d}[\mathbf{q}_i]\mathrm{d}[\mathbf{p}_i]}. \tag{1.7}$$

The final equations (1.5) are in an integro-differential form, which is ideal neither for numerical solutions nor for interpretation and further use. These issues will be confronted in the following section since the GENERIC formalism approaches the multiscale transition in a manner, which only operates with differential equations.

1.2 GENERIC

Another method of transition between levels of description (or rather transition between any key variables even on the same scale) is the GENERIC formalism (General Equation for Non-Equilibrium Reversible-Irreversible Coupling) [7]. This method combines two areas of mathematics for the evolution equations – the reversible dynamics, which is given by a poisson bracket with energy and the irreversible dynamics, which is described using a dissipation potential connected to entropy. In order to understand GENERIC, these two branches need to be elaborated on.

The main equation in GENERIC has the form [7]:

$$\dot{\mathrm{A}} = \{A, E\} + \left\langle \frac{\partial A}{\partial \mathbf{x}}, \frac{\partial \Xi}{\partial \mathbf{x}^*}\bigg|_{\mathbf{x}^*=S_{\mathbf{x}}}\right\rangle, \tag{1.8}$$

where $\{,\}$ is a Poisson bracket, $\langle,\rangle$ is a duality pairing, $\mathbf{x}^* = S_{\mathbf{x}} = \frac{\partial S}{\partial \mathbf{x}}$ are conjugate variables, $E(\mathbf{x})$ energy of the system and $\Xi = \Xi(\mathbf{x}, \mathbf{x}^*)$ is a dissipation potential.

In the special case of the state variables, Equation (1.8) gives:

$$\dot{x}^i = L^{ij}\frac{\partial E}{\partial x^j} + \frac{\partial \Xi}{\partial x_i^*}\bigg|_{\mathbf{x}^*=S_{\mathbf{x}}}. \tag{1.9}$$

On the left-hand side, there is the time derivative of the state variable x, e.g. position and momentum in the case of a canonical Hamiltonian systems, density

and velocity fields in the continuum mechanics or distribution density function if we want to reach the Liouville equation. On the right-hand side, the first term is the Poisson bracket of $\mathbf{x}$ with the energy of the system E. The Poisson bracket is written using the Poisson bivector, which is given as:

$$L^{ij} = \left\{ x^i, x^j \right\}$$

and together with the energy is the main ingredient for the description of the reversible dynamics. The second term is the gradient of dissipation potential as a function of conjugate variables, which are calculated as derivatives of entropy. For that reason, the second (irreversible) term requires the knowledge of the entropy as well as a dissipation potential of the studied system.

The poisson bracket builds on the geometric formulation of Hamiltonian mechanics. Since it represents the reversible evolution, the vanishment of the Poisson bracket means conservation in the reversible evolution. The Poisson bracket has four key properties: bilinearity, skew-symmetry, Leibniz rule and the Jacobi identity.

Skew-symmetry ($\{A, B\} = -\{B, A\}$) of the bivector ensures the conservation of energy:

$$\{E, E\} = -\{E, E\} = 0.$$

Both bilinearity and Leibniz rule mean that the bivector behaves as a derivative:

$$\{x, E + c\} = \{x, E\}, \quad c = const.,$$

i.e. a constant shift of energy does not change the reversible evolution. The Jacobi identity states:

$$\{A, \{B, C\}\} + \{B, \{C, A\}\} + \{C, \{A, B\}\} = 0$$

and warrants the conservation of the Poisson bracket throughout the reversible evolution as well as represents self-consistency of the evolution [7].

The irreversible dynamics stands fully on the dissipation potential Ξ. We expect it to satisfy three conditions.

First: the dissipation of total energy E has to be zero:

$$\left\langle \frac{\partial E}{\partial \mathbf{x}}, \left. \frac{\partial \Xi}{\partial \mathbf{x}^*} \right|_{\mathbf{x}^* = S_\mathbf{x}} \right\rangle = 0.$$

This carries the information, that GENERIC is a theory of closed systems. Any flows over the boundaries are delt with through boundary conditions.

Second: Ξ should be convex near $\mathbf{x}^* = 0$ for the dissipation to run towards the equilibrium at maximal entropy.

The third and last condition is the inequality:

$$\left. \mathbf{x}^* \frac{\partial \Xi}{\partial x_i^*} \right|_{\mathbf{x}^* = S_\mathbf{x}} \geq 0.$$

A sufficient condition is convexity of the dissipation potential. This inequality is one of the conditions for the second law of thermodynamics to hold within the formalism:

$$\dot{S} = \{S, E\} + \left\langle \frac{\partial S}{\partial \mathbf{x}}, \frac{\partial \Xi}{\partial \mathbf{x}^*} \Big|_{\mathbf{x}^* = S_\mathbf{x}} \right\rangle = 0 \;\; + \left\langle \mathbf{x}^*, \frac{\partial \Xi}{\partial \mathbf{x}^*} \Big|_{\mathbf{x}^* = S_\mathbf{x}} \right\rangle \geq 0. \qquad (1.10)$$

The first equality is using the evolution equation (1.8), the second equality notes that the entropy is a Casimir of the Poisson bracket (i.e. $\{S, \cdot\} = 0$) and the inequality is the third condition imposed on the dissipation potential.

As was mentioned before, the dissipation potential is a function of the conjugate variables $\mathbf{x}^*$ as well as the main variables $\mathbf{x}$. The relation between the variables $\mathbf{x}$ and the conjugate $\mathbf{x}^*$ is through the Legendre transform of entropy:

$$\frac{\partial}{\partial x^i} \left(-S + x^j x_j^* \right) = 0, \quad x_i^* = \frac{\partial S}{\partial x^i}, \quad \mathbf{x} = \mathbf{x}(\mathbf{x}^*). \qquad (1.11)$$

The use of differential geometry to describe the reversible evolution allows a simple transition between variables and thus also between different Poisson brackets:

$$\tilde{L}^{kl}(\mathbf{z}) = \frac{\partial z^k}{\partial x^i} L^{ij} \frac{\partial z^l}{\partial x^j}. \qquad (1.12)$$

An example of such transition is given in Section 2.4.

The transition between variables can be done even if it is between different levels of description. Within the GENERIC formalism there is a convention to call the more detailed description "upper" (denoted by $^\uparrow$) and the less detailed description "lower" (denoted by $^\downarrow$). When the transition goes from more upper to lower level of description, as was the case in the Mori-Zwanzig formalism, this transition leads to a loss of information. This loss does not intervene with Equation (1.12), that is to say the reversible evolution still undergoes the same transform. However, loss of information leads to change of entropy and change in the irreversible evolution. Finding the lower-level entropy is done through a static reduction – through the maximisation over the space of detailed variables (MaxEnt):

$$\frac{\partial}{\partial x^i} \left(-^\uparrow S + y^a(x) y_a^* \right) = 0, \quad \frac{\partial^\uparrow S}{\partial x^i} = y_a^* \frac{\partial \pi^a}{\partial x^i} \Big|_{\mathbf{x}(\mathbf{y}^*)}, \quad \mathbf{x} = \mathbf{x}(\mathbf{y}^*), \qquad (1.13)$$

where $y^a(x) = \pi^a(x)$ is a projection of the detailed variables on the less detailed ones. The function $\mathbf{x}(\mathbf{y}^*)$ is the submanifold of the manifold of the detailed variables, on which the upper entropy $^\uparrow S$ is maximised. An outcome of the MaxEnt procedure is the lower entropy as a function of the lower variables $^\downarrow S(\mathbf{y})$ as well as the entropy as a function of the conjugate lower variables $^\downarrow S^*(\mathbf{y})$. Transition between the two is through a full Legendre transform. An example of MaxEnt would be done in Section 2.2.

Even though in the GENERIC formalism the change of variables and the following transformation of the Poisson bivector are straightforward, finding the adequate dissipative potential is quite cumbersome. For that reason, we move to another form of multiscale transition – the lack-of-fit reduction.

1.3 The Lack-of-fit Reduction

The lack-of-fit reduction (or the optimal closure method) is another method of transition between detailed and resolved evolution. The method was first developed by Bruce Turkington [8, 9]. Since its creation up until now, the theory is still changing significantly. The core idea is staying unchanged – the relevant outcome of the optimal closure method is finding dissipative evolution for a given choice of resolved variables, which builds solely on the negligence of information from the underlying microscopic dynamics. In [9], this is studied for the case of Hamiltonian microscopic dynamics and both on the upper and lower level uses distribution functions – looking for "trial densities" as functions of the resolved variables. In its structure, the outcome resembles the GENERIC formalism introduced in the previous section. In [10], this resemblance is studied and formalised, using the lack-of-fit reduction in a generalised form. As the title of the article [10] suggests, the procedure starts with a GENERIC evolution (evolution with generalised reversible part and dissipation) and leads towards evolution again in GENERIC. Accordingly, we will use the same notation as in the previous section.

As was mentioned above, GENERIC is a formalism well equipped for the transition between levels of description, owing to its geometric structure (1.12). However, the maximisation of entropy does not give a satisfactory resolved evolution. It can be considered a static reduction, finding the correct conjugate variables and entropy on the less detailed level of description. For the evolution to transform correctly, a dynamical reduction is needed, which can project not only the detailed manifold to the resolved one, but also the tangent spaces of these manifolds [10]. The lack-of-fit reduction can be one of the methods for the dynamical reductions. It builds a lack-of-fit Lagrangian, which compares the upper with the lower evolution. The action created from this Lagrangian as an integral over time is then minimised over possible trajectories. Let us describe the process in more detail.

We will start with a GENERIC evolution (1.9) on the upper-level of description – the Poisson bivector $^\uparrow L^{ij}$ (or written as a bracket $^\uparrow\{\cdot,\cdot\}$), detailed variables x^i, the detailed dissipation potential $^\uparrow\Xi$, the detailed energy $^\uparrow E$ and the detailed entropy $^\uparrow S$ are known, together forming the upper evolution (1.9):

$$\dot{x}^i = {}^\uparrow\{x^i, {}^\uparrow E\} + \frac{\partial {}^\uparrow\Xi}{\partial x_i^*}\bigg|_{\mathbf{x}^* = \frac{\partial {}^\uparrow S}{\partial \mathbf{x}}}. \tag{1.14}$$

Afterwards, we choose the resolved variables $\mathbf{y}$. The relation of $\mathbf{y}$ to the detailed manifold is prescribed by a projection $\mathbf{y} = \pi(\mathbf{x})$. When looking for the lower evolution in the form (1.9), we require the projections to be linear in $\mathbf{x}$.

The resolved variables act as constraints for the maximalisation of the detailed entropy over the phase space of detailed variables – this is the static reduction outlined in Section 1.2. It leads to the lower level entropy $^\downarrow S(\mathbf{y})$ together with the lower level conjugate variables $\mathbf{y}^*$.

Our goal is the minimisation of information lost through the reduction. In other words, we aim to find the best approximation of the detailed evolution within the space of the lower variables. To find the information loss over the whole trajectory, we will first find the loss at specific time instance t. The lack-of-fit Lagrangian carries precisely this information. It is an entropy metric of

a residuum [10]. The entropy metric is the Hessian of upper entropy and the residuum is the difference between the upper and lower evolution:

$$R^i = \dot{x}^i - \frac{\partial x^i}{\partial y_a^*} \dot{y}_a^*.$$

An important element of the residuum is the description of the microscopic evolution $\dot{x}^i$. The residuum should lead us to the rate of the loss of information caused by the model reduction along the trajectory. In [9], the residuum is built on information theory and the Kullback-Leibler divergence, comparing a trial distribution to a distribution, which is an outcome of the Liouville equation, i.e. is a solution of the microscopic dynamics. Similarly to that, in [10] detailed GENERIC evolution is used and in that evolution instead of detailed energy (which would be a function of detailed variables) the apparent upper-level energy is used. It is found through a string of transitions between manifolds [10]:

$$^\uparrow \overline{E}(\mathbf{x}) \overset{\text{def}}{=} {}^\downarrow E\left({}^\downarrow \pi(\mathbf{x})\right) = {}^\uparrow E(\mathbf{x}(\mathbf{y}^*(\mathbf{y}(\mathbf{x})))). \tag{1.15}$$

Because the MaxEnt transition loses information, the mapping $\mathbf{x}(\mathbf{y}^*(\mathbf{y}(\mathbf{x})))$ is not simply equal to $\mathbf{x}$ and therefore $^\uparrow \overline{E}(\mathbf{x}) \neq {}^\uparrow E(\mathbf{x})$.

Having the upper evolution built as a flow given by the energy $^\uparrow \overline{E}$, i.e. $\dot{x}^i = {}^\uparrow\{x^i, {}^\uparrow \overline{E}\} = {}^\uparrow L^{ij}\frac{\partial^\uparrow \overline{E}}{\partial x^j} + \left.\frac{\partial^\uparrow \Xi}{\partial x_i^*}\right|_{\mathbf{x}^* = \frac{\partial^\uparrow S}{\partial \mathbf{x}}}$, allows us to write the residuum as a function of $\mathbf{y}^*$. This is an important motivation for the energy to have the form (1.15). The residuum therefore is:

$$R^i(\mathbf{x}(\mathbf{y}^*)) = {}^\uparrow L^{ij}\frac{\partial^\uparrow \overline{E}}{\partial x^j} + \left.\frac{\partial^\uparrow \Xi}{\partial x_i^*}\right|_{\mathbf{x}^* = \frac{\partial^\uparrow S}{\partial \mathbf{x}}} - \frac{\partial x^i}{\partial y_a^*} \dot{y}_a^*. \tag{1.16}$$

However, to be able to find the final evolution in the GENERIC form, we cannot simply make a Euclidean norm, as we will see later. This leads to the use of the aforementioned entropy metric. Another reason to use the entropy metric is the comparison to [9] and the expansion done within. Therefore, while searching for the lower GENERIC evolution we will use the lack-of-fit Lagrangian defined as:

$$\mathcal{L}(\mathbf{y}^*, \dot{\mathbf{y}}^*) = -\frac{1}{2}\left(R^i \frac{\partial^2 ({}^\uparrow S)}{\partial x^i \partial x^j} R^j\right). \tag{1.17}$$

Note that the matrix of second derivatives of entropy has to be negative definite, otherwise the entropy is not the correct entropy of the system. The negative definiteness of entropy leads to the convexity of the Lagrangian.

Finally, we formulate the optimisation principle [10, 9, 8]:

$$\psi(t_0, \mathbf{y}_0^*) = \min_{\mathbf{y}^*(t_0) = \mathbf{y}_0^*} \int\limits_{t_0}^{t_1} \mathrm{d}t \mathcal{L}(t, \mathbf{y}^*(t), \dot{\mathbf{y}}^*(t)), \tag{1.18}$$

where the fixed final state (at time $t_1 \to \infty$) is thought to be the equilibrium. This is a variational problem for free starting point and can be written as the Hamilton-Jacobi partial differential equation [11, 10]:

$$-\frac{\partial \psi}{\partial \mathbf{y}^*} = \frac{\partial \mathcal{L}}{\partial \dot{\mathbf{y}}^*} \Leftrightarrow \dot{\mathbf{y}}^* = \dot{\mathbf{y}}^*\left(\mathbf{y}^*, \frac{\partial}{\partial \mathbf{y}^*}\right), \tag{1.19a}$$

$$\frac{\partial \psi}{\partial t} = \mathcal{H}\left(t, \mathbf{y}^*, \frac{\partial \psi}{\partial \mathbf{y}^*}\right) = -\mathcal{L}\left(t, \mathbf{y}^*, \dot{\mathbf{y}}^*\left(\mathbf{y}^*, \frac{\partial}{\partial \mathbf{y}^*}\right)\right) - \frac{\partial \psi}{\partial \mathbf{y}^*}\dot{\mathbf{y}}^*\left(\mathbf{y}^*, \frac{\partial}{\partial \mathbf{y}^*}\right). \tag{1.19b}$$

We will expect the explicit dependence of ψ on t to disappear $\left(\frac{\partial \psi}{\partial t} = 0\right)$, thus placing the right-hand side of (1.19b) to zero. This corresponds to the expectation of large time scale separation between lower and upper variables [10].

Equation (1.19a) will lead to the lower evolution $\dot{\mathbf{y}}$ and (1.19b) has the function ψ as a solution. In order to find the evolution $\dot{\mathbf{y}}$, we require several intermediate steps. From (2.39) and (1.17):

$$\frac{\partial \mathcal{L}}{\partial \dot{y}_a^*} = \frac{\partial \mathcal{L}}{\partial R^i}\frac{\partial R^i}{\partial \dot{y}_a^*} = \frac{\partial^2(^\uparrow S)}{\partial x^i \partial x^j}R^j\frac{\partial x^i}{\partial y_a^*} = \left(^\uparrow L^{jk}\frac{\partial^\uparrow \overline{E}}{\partial x^k} + \frac{\partial^\uparrow \Xi}{\partial x_j^*}\bigg|_{\mathbf{x}^* = ^\uparrow S_{\mathbf{x}}} - \frac{\partial x^j}{\partial y_b^*}\dot{y}_b^*\right)\frac{\partial^2(^\uparrow S)}{\partial x^i \partial x^j}\frac{\partial x^i}{\partial y_a^*},$$

where we denoted $\frac{\partial^\uparrow S}{\partial \mathbf{x}} \equiv {}^\uparrow S_{\mathbf{x}}$.

Our goal is to formulate the evolution equation of $\mathbf{y}$ in a GENERIC form (1.9). There are three terms on the right-hand side of the equation above: the first term has the upper Liouville bivector and will become the reversible evolution, the second term will be an additional dissipative term caused by dissipation already present on the detailed level and the last term will be $\dot{\mathbf{y}}$ itself. The lower level dissipation potential as a solution of the Hamilton-Jacobi equation is on the left-hand side.

Using Equation (1.13), we may rewrite the first term as:

$$^\uparrow L^{jk}\frac{\partial^\uparrow \overline{E}}{\partial x^k}\frac{\partial^2(^\uparrow S)}{\partial x^i \partial x^j}\frac{\partial x^i}{\partial y_a^*} = \frac{\partial^\downarrow E}{\partial y^b}\frac{\partial y^b}{\partial x^k}{}^\uparrow L^{jk}\frac{\partial}{\partial y_a^*}\left(y_b^*\frac{\partial y^b}{\partial x^j}\right),$$

$$\frac{\partial}{\partial y_a^*}\left(y_b^*\frac{\partial y^b}{\partial x^j}\bigg|_{\mathbf{x}(\mathbf{y}^*)}\right) = \frac{\partial y^a}{\partial x^j} + y_b^*\frac{\partial y^b}{\partial y_a^* \partial y_c^*}\frac{\partial y_c^*}{\partial x^j},$$

we require the mapping $\pi^a(\mathbf{x}) = y^a$ to be linear, in order for the second term here to be zero. We arrive at:

$$\frac{\partial^\downarrow E}{\partial y^b}\frac{\partial y^b}{\partial x^k}{}^\uparrow L^{jk}\frac{\partial y^a}{\partial x^j} \equiv {}^\downarrow L^{ab}\frac{\partial^\downarrow E}{\partial y^b} = {}^\downarrow\{y^a, {}^\downarrow E\}.$$

Proceeding with the second term:

$$\frac{\partial^\uparrow \Xi}{\partial x_j^*}\bigg|_{\mathbf{x}^* = ^\uparrow S_{\mathbf{x}}}\frac{\partial^2(^\uparrow S)}{\partial x^i \partial x^j}\frac{\partial x^i}{\partial y_a^*} = \frac{\partial^\uparrow \Xi}{\partial x_j^*}\bigg|_{\mathbf{x}^* = ^\uparrow S_{\mathbf{x}}}\frac{\partial x_j^*}{\partial x^i}\frac{\partial x^i}{\partial y_a^*} = \frac{\partial^\uparrow \Xi}{\partial x_j^*}\bigg|_{\mathbf{x}^* = ^\uparrow S_{\mathbf{x}}}\frac{\partial x_j^*}{\partial y_a^*}$$

and finally the third term:

$$\frac{\partial x^j}{\partial y_b^*}\dot{y}_b^*\frac{\partial^2(^\uparrow S)}{\partial x^i \partial x^j}\frac{\partial x^i}{\partial y_a^*} = \dot{y}_b^*\frac{\partial^2(^\downarrow S^*)}{\partial y_a^* \partial y_b^*} = \frac{dy_b^*}{dt}\frac{\partial y^a}{\partial y_b^*} = \dot{y}^a.$$

Using these adjustments, we can write the lower evolution equation from (1.19a):

$$\dot{y}^a = {}^{\downarrow}\{y^a, {}^{\downarrow}E\} + \frac{\partial}{\partial y_a^*}\left[{}^{\uparrow}\Xi\left(\mathbf{x}^*(\mathbf{y}^*), \mathbf{x}(\mathbf{y})\right) + \psi(\mathbf{y}^*)\right]. \qquad (1.20)$$

We are writing here ${}^{\uparrow}\Xi\left(\mathbf{x}^*(\mathbf{y}^*), \mathbf{x}(\mathbf{y})\right)$ since the GENERIC formalism, unlike the lack-of-fit reduction, works with a dissipation potential dependent in general on both $\mathbf{x}^*$ and $\mathbf{x}$.

Before reviewing the whole process of the optimal closure method, we will first make a review of one of the approaches to solving the Hamilton-Jacobi equation.

1.3.1 The Riccati Equation

For a quadratic Hamiltonian, a quadratic ansatz $\psi = \frac{1}{2}\mathbf{y}^*\mathbb{M}\mathbf{y}^*$ leads to a Riccati type of equation. In this section, we will focus on finding the solutions of the Riccati equation and its behaviour, using [12] as our source for the definitions and theorems. We will assume that $\mathbb{M}$ is not a function of time and the Ricatti equation is, therefore, an algebraic equation for the matrix $\mathbb{M}$:

$$0 = -\mathbb{M}\mathbb{P}\mathbb{M} + \mathbb{M}\mathbb{B} + \mathbb{B}^T\mathbb{M} + \mathbb{Q}. \qquad (1.21)$$

Following [12], we will also be working with the matrix $\mathbb{P}$ in a form $\mathbb{P} = \mathbb{A}\mathbb{A}^T$ and similarly with the matrix $\mathbb{Q}$ in a form $\mathbb{Q} = \mathbb{C}\mathbb{C}^T$.

One of the properties of the dissipation potential is convexity (1.10) and for that reason we are searching for a non-negative solution of the Riccati equation. The properties of such solution are summarised in [12] and we will be using only the results found therein.

Definition 1 (Unobservable eigenvalue). *It is said to be unobservable eigenvalue of the pair the pair ($\mathbb{C}$,$\mathbb{B}$) if there exists a nontrivial right eigenvector $\mathbf{z}$ of $\mathbb{B}$ with the eigenvalue λ such that it lies in the kernel of $\mathbb{C}$, i.e. $\mathbb{B}\mathbf{z} = \lambda\mathbf{z}$ and $\mathbb{C}\mathbf{z} = 0$.*

Definition 2. *The pair ($\mathbb{B}$,$\mathbb{A}$) is said to be stabilazable if a matrix over $\mathbb{R}$ exists such that $\mathbb{B} + \mathbb{A}\mathbb{L}$ is stable (i.e., all its eigenvalues have negative real parts).*

Definition 3. *The pair ($\mathbb{C}$,$\mathbb{B}$) is said to be detectable if the unstable eigenvalues of ($\mathbb{C}$,$\mathbb{B}$) are observable.*

The existence and uniqueness of stabilising solutions abide by the following theorems [12].

Theorem 1. *The stabilising solution of (1.21) exists if and only if ($\mathbb{B}$,$\mathbb{A}$) is stabilizable and the real part of all eigenvalues of $\mathbb{M}$ is different from zero.*

Theorem 2. *The stabilising solution is the only nonnegative solution of (1.21) if and only if ($\mathbb{C}$, $\mathbb{B}$) is detectable.*

The proofs of these theorems can be found in [12].

1.3.2 The Lack-of-fit Procedure

After this technical detour, let us give a short summary – a step-by-step procedure of the optimal closure method:

1. Formulate the upper evolution (1.14), i.e. variables $\mathbf{x}$, detailed energy $^{\uparrow}E$, Poisson bivector $^{\uparrow}L$, dissipation potential $^{\uparrow}\Xi$ and the detailed entropy $^{\uparrow}S$.

2. State the projection to the lower-level variables $\pi(\mathbf{x}) = \mathbf{y}$, in other words choose the resolved variables as functions of $\mathbf{x}$.

3. Do the static reduction (1.13), i.e. maximise the entropy $^{\uparrow}S$ over the space of detailed variables $\mathbf{x}$ with the resolved variables $\mathbf{y}^a$ acting as constraints.

4. Find the apperent upper-level energy $^{\uparrow}\overline{E}$ from (1.15).

5. Find the residuum R from (2.39).

6. Find the Lagrangian $\mathcal{L}$ from (1.17).

7. Obtain $\dot{\mathbf{y}}^*$ as a function of $\mathbf{y}^*$ and $\frac{\partial \psi}{\partial \mathbf{y}^*}$ from (1.19a).

8. Write the Hamiltonian $\mathcal{H}$, formulate the Hamilton-Jacobi equations for ψ and solve (1.19b).

9. Formulate the evolution $\dot{\mathbf{y}}$ from (1.20).

1.4 Summary

We have introduced two methods of transition between physical scales. The first was the Mori-Zwanzig formalism in Section 1.1 and the second was the lack-of-fit reduction in Section 1.3, formulated within the GENERIC formalism, reviewed in Section 1.2.

The Mori-Zwanzig formalism starts with a set of differential equations and uses a projector to reduce the number of equations to only a set of evolution equations, which correspond to some resolved variables. The evolution of the resolved variables is described by integro-differential equations. These equations carry the same information as the detailed differential equations we began with. However, the integro-differential equations can be further simplified through various approximations. They are therefore a stepping stone for a dimensional reduction.

Before outlying the second method of dimensional reduction, we introduced the GENERIC formalism in Section 1.2. It is a geometric way of system description, wherein the evolution is split into a time-reversible and time-irreversible term. The reversible term is result of a Poisson bracket with energy of the system and the irreversible term is a duality pairing with a gradient of dissipation potential. In other words, the reversible evolution is governed by the total energy of the system and the geometry of the Poisson bracket, whereas the irreversible part is governed by the entropy and the dissipation in the system.

When transitioning from upper (detailed) to less lower (detailed) level of description, a dissipation potential needs to be found.The lack-of-fit reduction (or the optimal closure method) introduced in Section 1.3 is an attempt to do as

such. When applied on upper evolution formulated using GENERIC, it leads to a set of differential equations, again in a GENERIC form, with a dissipation potential as a result of the procedure. These lower evolution equations are an outcome of minimisation of the lack-of-fit Lagrangian. The lack-of-fit Lagrangian is built from an entropy metric (the Hessian of the upper entropy) and a residuum. The residuum is the difference between detailed evolution, formulated in entropy conjugate lower variables ($\mathbf{y}^* = \frac{\partial^\downarrow S}{\partial \mathbf{y}}$), and the lower evolution again within the conjugate variables. This minimisation leads to the Hamilton-Jacobi equation for the sought-after dissipation potential and also the evolution of the lower variables. In the last subsection, we outlined steps to be followed when using the lack-of-fit reduction.

2. The Kac-Zwanzig Model

The Kac-Zwanzig model represents a particle inside a heat bath and as such it is a system of N+1 classical particles without further inner dimensions of freedom. Closer study of this system was done already in [13]. The particles are separated into two groups – one distinguished particle with mass M and N small particles with masses m_i. We will also refer to the small particles as "the cloud". The cloud is connected to the distinguished particle with springs, i.e. the harmonic potential. Each spring can have different stiffness parameter k_i. For simplicity we will assume stiffness $\frac{\gamma}{N}$ for all particles of the cloud. For growing number of particles in the cloud, the stiffness will decrease and thus the energy will be somehow bounded. Furthermore, the distinguished particle can be influenced by an outside potential $V(Q)$. The Hamiltonian of such system therefore is:

$$H = \frac{P^2}{2M} + V(\mathbf{Q}) + \sum_{i=1}^{N} \left[\frac{p_i^2}{2m_i} + \frac{\gamma}{2N} \left(\mathbf{q}_i - \mathbf{Q} \right)^2 \right], \tag{2.1}$$

where $\mathbf{Q}, \mathbf{P}$ is the position and momentum of the distinguished particle and $\{\mathbf{q}_i, \mathbf{p}_i\}_{i=1}^{N}$ are positions and momenta of the undistinguished particles. The vectors of positions and momenta can have an arbitrary dimension d and therefore the detailed phase space is $\mathbb{R}^{d(N+1)}$. The detailed manifold can also be the space of the distribution functions, as will be the case in Chapter 2.2.

Throughout this chapter we will be using different notations, depending on convenience of the calculations. We will be consistent in the following definitions:

$$\mathbf{s} \equiv \frac{1}{N} \sum_{i=1}^{N} \mathbf{q}_i - \mathbf{Q}, \qquad \omega_i^2 = \frac{\gamma}{m_i N}, \qquad \mathrm{d}\mathbf{q}_i \mathrm{d}\mathbf{p}_i, = \mathrm{d}\mathbf{i}, \qquad \mathrm{d}\mathbf{1}...\mathrm{d}\mathbf{N} = \mathrm{d}[\mathbf{j}].$$

2.1 The Mori-Zwanzig Formalism

We will now apply the Mori Zwanzig formalism on the Kac-Zwanzig model. As was suggested during the introduction of the projectors, we will consider two choices of resolved variables: position and momentum of the distinguished particle $(\mathbf{Q}, \mathbf{P})$ and in the second choice above the two also the mean distance from the cloud $(\mathbf{Q}, \mathbf{P}, \mathbf{s})$.

To describe the evolution we require the Liouvillian L of the system and a projector $\mathcal{P}$. The Liouvillian is independent on the choice of the resolved variables since it exists on the detailed manifold:

$$L = \frac{\mathbf{P}}{M} \frac{\partial}{\partial \mathbf{Q}} - \left[V'(\mathbf{Q}) - \gamma \mathbf{s} \right] \frac{\partial}{\partial \mathbf{P}} + \sum_{i=1}^{N} \left[\frac{\mathbf{p}_i}{m_i} \frac{\partial}{\partial \mathbf{q}_i} - \frac{\gamma}{N} \left(\mathbf{q}_i - \mathbf{Q} \right) \frac{\partial}{\partial \mathbf{p}_i} \right]. \tag{2.2}$$

The Liouvillian acts on the positions and momenta of all $(N+1)$ particles in the following manner:

$$L\mathbf{Q} = \frac{\mathbf{P}}{M}, \qquad\qquad L\mathbf{P} = -V' + \gamma\mathbf{s}, \qquad\qquad (2.3\text{a})$$

$$L\mathbf{q}_i = \frac{\mathbf{p}_i}{m_i}, \qquad\qquad L\mathbf{p}_i = -\frac{\gamma}{N}(\mathbf{q}_i - \mathbf{Q}). \qquad\qquad (2.3\text{b})$$

The projectors are dependent on our choice of the resolved variables: in the case $(\mathbf{Q}, \mathbf{P})$ we will be using the form written in Equation (1.6) and for $(\mathbf{Q}, \mathbf{P}, \mathbf{s})$ we will use the form from Equation (1.7).

First let us focus on the resolved variables $(\mathbf{Q}, \mathbf{P})$. From the evolution equations (1.3) and (1.5), we see that the relevant projections are $\mathcal{P}\mathbf{Q}$, $\mathcal{P}\mathbf{P}$, $\mathcal{P}\mathbf{q}_i$ and $\mathcal{P}\mathbf{p}_i$. For any $f = f(\mathbf{Q}, \mathbf{P})$, the projector is:

$$\mathcal{P}f(\mathbf{Q}, \mathbf{P}) = \frac{\int f e^{-\beta H} \mathrm{d}[\mathbf{i}]}{\int e^{-\beta H} \mathrm{d}[\mathbf{i}]} = f\frac{\int e^{-\beta H} \mathrm{d}[\mathbf{i}]}{\int e^{-\beta H} \mathrm{d}[\mathbf{i}]} = f,$$

as is expected since these variables are what we project on. The projection $\mathcal{P}\mathbf{p}_i$ gives zero for all i, because the Hamiltonian is even in $\mathbf{p}_i$. $\mathcal{P}\mathbf{q}_i$ can be calculated using the fact, that the Hamiltonian is even in $(\mathbf{q}_i - \mathbf{Q})$ and the projector $\mathcal{P}$ is linear:

$$\mathcal{P}(\mathbf{q}_i - \mathbf{Q}) = 0 \iff \mathcal{P}\mathbf{q}_i = \mathcal{P}\mathbf{Q} = \mathbf{Q}.$$

To project on $\mathbf{Q}, \mathbf{P}$ and $\mathbf{s}$, we will use the projector (1.7) and denote it as $\mathcal{P}_s$. The key projections are $\mathcal{P}_s\mathbf{Q}$, $\mathcal{P}_s\mathbf{P}$, $\mathcal{P}_s\mathbf{q}_i$, $\mathcal{P}_s\mathbf{p}_i$ and also $\mathcal{P}_s\left(\frac{1}{N}\sum_j(\mathbf{q}_j - \mathbf{Q})\right) = \mathcal{P}_s\mathbf{s}$.

Similarly as before, any function $f = f(\mathbf{Q}, \mathbf{P}, \mathbf{s})$ projects onto itself and $\mathcal{P}_s\mathbf{p}_i = 0$. The last projector to be calculated is $\mathcal{P}_s\mathbf{q}_i$. For that we need to calculate two very similar integrals (the nominator and denominator of $\mathcal{P}_s$). We will calculate them together and colour-code the additional $\mathbf{q}_i$ in the numerator with red. All multiplicative factors that can be canceled out, will be first colour-coded blue and then omitted. With that, let us calculate the projection:

$$\int \mathbf{q}_i e^{-\beta\left[\frac{P^2}{2M} + V(Q) + \sum_{j=1}^{N}\frac{p_j^2}{2m_j} + \frac{\gamma}{2N}(\mathbf{q}_j - \mathbf{Q})^2\right]} \delta\left(\frac{1}{N}\sum_j(\mathbf{q}_j - \mathbf{Q}) - \mathbf{s}\right)\mathrm{d}[\mathbf{j}],$$

$$\int \mathbf{q}_i e^{-\beta\sum_{j=1}^{N}\frac{\gamma}{2N}(\mathbf{q}_j - \mathbf{Q})^2} \delta\left(\frac{1}{N}\sum_j(\mathbf{q}_j - \mathbf{Q}) - \mathbf{s}\right)\mathrm{d}[\mathbf{q}_j].$$

We can integrate over one of the particles, i.e. over some q_k, $k \neq i$ and therefore make use of the delta function $\delta\left(\frac{1}{N}\sum_j(\mathbf{q}_j - \mathbf{Q}) - s\right)$:

$$\frac{1}{N}\sum_j(\mathbf{q}_j - \mathbf{Q}) - \mathbf{s} = 0 \iff \mathbf{q}_k - \mathbf{Q} = N\mathbf{s} - \sum_{j\neq k}(\mathbf{q}_j - \mathbf{Q}),$$

$$\int \mathbf{q}_i e^{-\frac{\beta\gamma}{2N}\left[N^2\mathbf{s}^2 - 2N\mathbf{s}\sum_{j\neq k}(\mathbf{q}_j - \mathbf{Q}) + \left(\sum_{j\neq k}(\mathbf{q}_j - \mathbf{Q})\right)^2 + \sum_{j\neq k}(\mathbf{q}_j - \mathbf{Q})^2\right]}\mathrm{d}[\mathbf{q}_j]_{j\neq k} \propto$$

$$\propto \int \mathbf{q}_i e^{-\frac{\beta\gamma}{2N}\left[-2N\mathbf{s}\sum_{j\neq k}(\mathbf{q}_j - \mathbf{Q}) + \sum_{j\neq k}(\mathbf{q}_j - \mathbf{Q})^2\right]}\exp\left(-\frac{1}{2}\left(\sqrt{\frac{\beta\gamma}{N}}\sum_{j\neq k}(\mathbf{q}_j - \mathbf{Q})\right)^2\right)\mathrm{d}[\mathbf{q}_j]_{j\neq k}.$$

Using the Hubbard-Stratonovich formula [14]:

$$\exp\left(-\frac{1}{2}\mathbf{x}^2\right) = \frac{1}{\sqrt{2\pi}}\int\limits_{-\infty}^{\infty}\exp\left(-\frac{y^2}{2} - i\mathbf{x}\cdot\mathbf{y}\right)\,\mathrm{d}\mathbf{y},$$

we proceed with the calculations

$$\int \mathbf{q}_i e^{-\frac{\beta\gamma}{2N}\left[\sum\limits_{j\neq k}(\mathbf{q}_j-\mathbf{Q})^2 + 2\left(-N\mathbf{s}+i\mathbf{y}\sqrt{\frac{N}{\beta\gamma}}\right)\cdot\sum\limits_{j\neq k}(\mathbf{q}_j-\mathbf{Q})\right]}e^{-\frac{y^2}{2}}\,\mathrm{d}[\mathbf{q}_j]_{j\neq k}\mathrm{d}\mathbf{y} =$$

$$\int \mathbf{q}_i e^{-\frac{\beta\gamma}{2N}\sum\limits_{j\neq k}\left[\mathbf{q}_j-\mathbf{Q}-N\mathbf{s}+i\mathbf{y}\sqrt{\frac{N}{\beta\gamma}}\right]^2}e^{-\frac{y^2}{2}+\frac{\beta\gamma(N-1)}{2N}\left(-N\mathbf{s}+i\mathbf{y}\sqrt{\frac{N}{\beta\gamma}}\right)^2}\,\mathrm{d}[\mathbf{q}_j]_{j\neq k}\mathrm{d}\mathbf{y} \propto$$

$$\propto \int \mathbf{q}_i e^{-\frac{\beta\gamma}{2N}\sum\limits_{j\neq k}\left[\mathbf{q}_j-\mathbf{Q}-N\mathbf{s}+i\mathbf{y}\sqrt{\frac{N}{\beta\gamma}}\right]^2}e^{-\frac{N}{2}\left(\mathbf{y}+i(N-1)\sqrt{\frac{\beta\gamma}{N}}\mathbf{s}\right)^2}\,\mathrm{d}[\mathbf{q}_j]_{j\neq k}\mathrm{d}\mathbf{y} \; .$$

We will now substitute $\Delta_y = \mathbf{y} + i(N-1)\sqrt{\frac{\beta\gamma}{N}}\mathbf{s}$, $\Delta_j = \mathbf{q}_j - \mathbf{Q} - \mathbf{s} + i\Delta_y\sqrt{\frac{N}{\beta\gamma}}$ and the exponential of sum will change to a product of exponentials:

$$\int\left(\Delta_j + \mathbf{Q} + \mathbf{s} - i\Delta_y\sqrt{\frac{N}{\beta\gamma}}\right)\prod_{j\neq k}e^{-\frac{\beta\gamma}{2N}\Delta_j^2}e^{-\frac{N}{2}\Delta_y^2}\mathrm{d}[\Delta_j]_{j\neq k}\mathrm{d}\Delta_y \; .$$

Terms $\left(\Delta_j - i\Delta_y\sqrt{\frac{N}{\beta\gamma}}\right)$ give zero (integrating an odd function over the whole space) and $(\mathbf{Q}+\mathbf{s})$ are constant under the integration, thus the Gassian integrals give only a factor which will cancel in the projector. This leads us to the result:

$$\mathcal{P}_s\mathbf{q}_i = \mathbf{Q} + \mathbf{s} \; .$$

To sum up, the projectors are:

$$\mathcal{P}f(\mathbf{Q},\mathbf{P}) = f(\mathbf{Q},\mathbf{P}), \qquad \mathcal{P}\mathbf{q}_i = \mathbf{Q}, \qquad \mathcal{P}\mathbf{p}_i = 0, \qquad (2.4\mathrm{a})$$

$$\mathcal{P}_sf(\mathbf{Q},\mathbf{P},\mathbf{s}) = f(\mathbf{Q},\mathbf{P},\mathbf{s}), \qquad \mathcal{P}_s\mathbf{q}_i = \mathbf{Q} + \mathbf{s}, \qquad \mathcal{P}_s\mathbf{p}_i = 0. \qquad (2.4\mathrm{b})$$

Using this result, we write the orthogonal evolution equation (1.3) for the two different choices of projections:

$$\frac{\partial}{\partial t}S_\perp^t\mathbf{Q} = 0, \qquad (2.5\mathrm{a})$$

$$\frac{\partial}{\partial t}S_\perp^t\mathbf{P} = \frac{\gamma}{N}\sum_j\left(S_\perp^t\mathbf{q}_j - S_\perp^t\mathbf{Q}\right), \qquad (2.5\mathrm{b})$$

$$\frac{\partial}{\partial t}S_\perp^t\mathbf{q}_i = \frac{S_\perp^t\mathbf{p}_i}{m_i}, \qquad (2.5\mathrm{c})$$

$$\frac{\partial}{\partial t}S_\perp^t\mathbf{p}_i = -\frac{\gamma}{N}\left(S_\perp^t\mathbf{q}_i - S_\perp^t\mathbf{Q}\right), \qquad (2.5\mathrm{d})$$

$$\frac{\partial}{\partial t} S_\perp^t \mathbf{Q} = 0, \tag{2.6a}$$

$$\frac{\partial}{\partial t} S_\perp^t \mathbf{P} = 0, \tag{2.6b}$$

$$\frac{\partial}{\partial t} S_\perp^t \mathbf{q}_i = \frac{S_\perp^t \mathbf{p}_i}{m_i}, \tag{2.6c}$$

$$\frac{\partial}{\partial t} S_\perp^t \mathbf{p}_i = -\frac{\gamma}{N} \left(S_\perp^t \mathbf{q}_i - S_\perp^t \mathbf{Q} - S_\perp^t \mathbf{s} \right), \tag{2.6d}$$

$$\frac{\partial}{\partial t} S_\perp^t \mathbf{s} = \frac{1}{N} \sum_{i=1}^{N} \frac{S_\perp^t \mathbf{p}_i}{m_i}. \tag{2.6e}$$

In Equation (2.5) is the orthogonal evolution with projection onto $\mathbf{Q}$ and $\mathbf{P}$, in Equation (2.6) is the orthogonal evolution with the projection onto $\mathbf{Q}$, $\mathbf{P}$ and $\mathbf{s}$.

For the final evolution equation (1.5), it is necessary to calculate the orthogonal evolution of the function, which was denoted by $\mathbf{F}$. When looking for evolution of $(\mathbf{Q}, \mathbf{P})$, this function consists of the right-hand side of equations (2.5a) and (2.5b), first of which is zero. Therefore only the orthogonal evolution of $\mathbf{Q}$ and $\mathbf{q}_i, \forall i$ needs to be calculated.

Equation (2.5a) states, that for the orthogonal evolution the variable $\mathbf{Q}$ is constant and equal to the initial condition:

$$S_\perp^t \mathbf{Q} = \mathbf{Q}.$$

Equation (2.5c) and (2.5d) are a set of $d \cdot N$ equations for decoupled harmonic oscillators with intrinsic frequencies ω_i:

$$S_\perp^t \mathbf{q}_i = \frac{\mathbf{p}_i \omega_i N}{\gamma} \sin(\omega_i t) + (\mathbf{q}_i - \mathbf{Q}) \cos(\omega_i t) + \mathbf{Q}.$$

The coefficients in front of the goniometric functions are calculated from the initial conditions. As a result, the function of the force $S_\perp^t \mathbf{F}$ is:

$$S_\perp^t \mathbf{F} = \sum_{i=1}^{N} \left(\omega_i \mathbf{p}_i \sin(\omega_i t) + \frac{\gamma}{N} (\mathbf{q}_i - \mathbf{Q}) \cos(\omega_i t) \right) \tag{2.7}$$

and the memory-kernel function is:

$$\mathcal{P} L S_\perp^t \mathbf{F} = -\frac{\gamma}{NM} \sum_{i=1}^{N} \cos(\omega_i t) \mathbf{P}. \tag{2.8}$$

For the resolved variables $(\mathbf{Q}, \mathbf{P}, \mathbf{s})$, the random force $\mathbf{F}$ will consist of the right-hand side of Equation (2.6a), (2.6b) and (2.6e). We only need the orthogonal evolution $S_\perp^t \mathbf{p}_i, \forall i$ because the right hand sides of Equation (2.6a) and (2.6b) are zero. A straight forward calculation gives:

$$S_\perp^t \mathbf{Q} = \mathbf{Q}, \quad S_\perp^t \left(\mathbf{s} - \frac{1}{N} \sum_{j=1}^{N} \mathbf{q}_j \right) = \mathbf{s} - \frac{1}{N} \sum_{j=1}^{N} \mathbf{q}_j = -\mathbf{Q},$$

but every other step in finding the necessary evolution requires the solution of a non-trivial system of differential equations, albeit with constant coefficients. The

following subsection will contain detailed calculation of the orthogonal evolution $\frac{1}{N}\sum_{i=1}^{N}\frac{S_\perp^t\mathbf{p}_i}{m_i}$. Subsection 2.1.2 will summarise the final evolution equations for both choices of resolved variables.

2.1.1 Computational Intermezzo

Equation (2.6c) and (2.6d) can be reformulated as a system of second order ODEs (Ordinary Differential Equations):

$$\frac{\partial^2}{\partial t^2}S_\perp^t\mathbf{p}_i = -S_\perp^t(\omega_i^2\mathbf{p}_i) + \frac{1}{N}\sum_{j=1}^{N}S_\perp^t(\omega_j^2\mathbf{p}_j).$$

For the calculations done in this subsection, we will write $S_\perp^t\mathbf{p}_i = \mathbf{p}_i(t)$ since we will not be using any different evolution operator. The initial conditions will be denoted by the subscript 0, i.e. $\mathbf{p}_{0i}$. Thus we may write $\mathbf{p}_i(t) = \mathbf{p}_i$ and

$$\ddot{\mathbf{p}}_i = -\omega_i^2\mathbf{p}_i + \frac{1}{N}\sum_{j=1}^{N}\omega_j^2\mathbf{p}_j.$$

By applying the Laplace transform $\mathcal{L}\mathbf{p}_i = \hat{\mathbf{p}}_i(\omega)$, we acquire from Equation (2.6) a set of algebraic equations for $\hat{\mathbf{p}}_i$:

$$\begin{pmatrix} \omega^2 + \omega_1^2 - \frac{\omega_1^2}{N} & -\frac{\omega_2^2}{N} & \cdots & -\frac{\omega_N^2}{N} \\ -\frac{\omega_1^2}{N} & \omega^2 + \omega_2^2 - \frac{\omega_2^2}{N} & \cdots & -\frac{\omega_N^2}{N} \\ \vdots & \vdots & \ddots & \vdots \\ -\frac{\omega_1^2}{N} & -\frac{\omega_2^2}{N} & \cdots & \omega^2 + \omega_N^2 - \frac{\omega_N^2}{N} \end{pmatrix}\begin{pmatrix} \hat{\mathbf{p}}_1 \\ \hat{\mathbf{p}}_2 \\ \vdots \\ \hat{\mathbf{p}}_N \end{pmatrix} = \begin{pmatrix} \mathbf{b}_1 \\ \mathbf{b}_2 \\ \vdots \\ \mathbf{b}_N \end{pmatrix}, \qquad (2.9)$$

with $\mathbf{b}_i = \omega\mathbf{p}_{0i} - \frac{\gamma}{N}\left(\mathbf{q}_{0i} - \mathbf{s}_0 - \mathbf{Q}_0\right)$ since $\dot{\mathbf{p}}_i\big|_{t=0} = -\frac{\gamma}{N}\left(\mathbf{q}_{0i} - \mathbf{s}_0 - \mathbf{Q}_0\right)$. Note that we have in general $d \cdot N$ equations, even though at no point we will require to focus on any specific element of a single vector $\mathbf{p}_i$. This leads us to write e.g. $\omega^2 + \omega_1^2 - \frac{\omega_1^2}{N}$ instead of $(\omega^2 + \omega_1^2 - \frac{\omega_1^2}{N})\mathbb{I}$, with $\mathbb{I}$ being the identity matrix in $\mathbb{R}^{d\times d}$.

We can add up all the rows, which will give us an equation

$$\frac{1}{N}\sum_{j=1}^{N}\hat{\mathbf{p}}_j = \frac{\frac{1}{N}\sum_{j=1}^{N}\mathbf{p}_{0j}}{\omega}, \qquad (2.10)$$

in other words this is the conservation of momentum in the orthogonal evolution (since $\mathcal{L}^{-1}(\frac{1}{\omega}) = 1$, $t \geq 0$).

For easier manipulation, let us denote

$$\Omega_i \equiv \omega^2 + \omega_i^2, \qquad \overline{\mathbf{p}}_0 \equiv \frac{1}{N}\sum_{j=1}^{N}\mathbf{p}_{0j}, \qquad x_{0j} \equiv \omega\mathbf{p}_{0j} - \frac{\gamma}{N}\mathbf{q}_{0j}. \qquad (2.11)$$

Furthermore, we may order the random frequencies so that $\omega_1^2 \geq \omega_2^2 \geq ... \geq \omega_N^2$.

18

To find the solution, we will use the observation that the difference of any two rows is:

$$\Omega_j \hat{\mathbf{p}}_j - \Omega_i \hat{\mathbf{p}}_i = x_{0j} - x_{0i}.$$

Substituting $\hat{\mathbf{p}}_j$ in Equation (2.10) will give us the solution for $\hat{\mathbf{p}}_i$:

$$\hat{\mathbf{p}}_i = \frac{\frac{\overline{\mathbf{p}}_0}{\omega} - \frac{1}{N}\sum_{j=1}^{N}\frac{x_{0j}-x_{0i}}{\Omega_j}}{\frac{1}{N}\sum_{j=1}^{N}\frac{\Omega_i}{\Omega_j}} = \frac{\overline{\mathbf{p}}_0}{\omega}\frac{1}{\frac{1}{N}\sum_{j=1}^{N}\frac{\Omega_i}{\Omega_j}} - \frac{\frac{1}{N}\sum_{j=1}^{N}\frac{x_{0j}}{\Omega_j}}{\frac{1}{N}\sum_{j=1}^{N}\frac{\Omega_i}{\Omega_j}} + \frac{x_{0i}}{\Omega_i}. \qquad (2.12)$$

Next step is to find the inverse Laplace transform of $\hat{\mathbf{p}}_i$. It is useful to rewrite the equality (2.12) using $\hat{A}_{k;j}$ given by:

$$\hat{A}_{k;j} = \frac{\omega^k}{\Omega_j}\frac{1}{\frac{1}{N}\sum_{i=1}^{N}\frac{1}{\Omega_i}} = \frac{\omega^k}{(\omega^2 + \omega_j^2)}\frac{\prod_{i=1}^{N}\left(\omega^2 + \omega_i^2\right)}{Q(\omega^2)}, \;\; k = -1, 0, 1,$$

where $Q(\omega^2)$ is a polynomial with $N-1$ roots. The roots will be denoted by $(i\omega_{Ql})^2 = -(\omega_{Ql})^2$, i.e.

$$Q(\omega^2) \equiv \frac{1}{N}\sum_{j=1}^{N}\frac{\prod_{i=1}^{N}(\omega^2 + \omega_i^2)}{\omega^2 + \omega_j^2} = \prod_{l=1}^{N-1}(\omega^2 + \omega_{Ql}^2).$$

As a consequence of our definition, the following equality holds

$$\sum_{j=1}^{N}\hat{A}_{k;j} = N\omega^k \qquad (2.13)$$

and we arrive at the solution in the Laplace picture:

$$\hat{\mathbf{p}}_i = \frac{\omega\mathbf{p}_{0i} - \frac{\gamma}{N}\mathbf{q}_{0i}}{\omega^2 + \omega_i^2} + \overline{\mathbf{p}}_0\hat{A}_{-1;i} - \frac{1}{N}\sum_{j=1}^{N}\frac{\mathbf{p}_{0j}\hat{A}_{1;i} - \frac{\gamma}{N}\mathbf{q}_{0j}\hat{A}_{0;i}}{\omega^2 + \omega_j^2}.$$

All terms are rational functions of ω, with higher order polynomials in the numerator. The inverse Laplace transform of such rational functions is found as [15]:

$$\mathcal{L}^{-1}(F) = \sum_{i=1}^{n}\mathrm{res}_{a_i}\left[F(\omega)e^{\omega t}\right]$$

with n being the number of poles.
In our case the F has several different forms.

The first form is $F = \frac{\omega \mathbf{p}_{0i} - \frac{\gamma}{N}\mathbf{q}_{0i}}{\omega^2 + \omega_i^2}$:

$$\mathcal{L}^{-1}(F) = \mathbf{p}_{0i}\cos(\omega_i t) - \frac{\gamma}{N}\mathbf{q}_{0i}\frac{\sin(\omega_i t)}{\omega_i}.$$

The second term is $F = \overline{\mathbf{p}}_0 \hat{A}_{-1;i}$ and using

$$\hat{A}_{-1;i}\omega\bigg|_{\omega=0} = \frac{1}{\frac{1}{N}\sum\limits_{j=1}^{N}\frac{(\omega^2+\omega_i^2)}{(\omega^2+\omega_j^2)}}\bigg|_{\omega=0} = \frac{1}{\omega_i^2}\frac{1}{\frac{1}{N}\sum\limits_{j=1}^{N}\frac{1}{\omega_j^2}} = \frac{\gamma}{\omega_i^2 N}\frac{1}{\overline{m}},$$

with $\overline{m} = \frac{1}{N}\sum\limits_{j=1}^{N} m_j$, we calculate the inverse as:

$$\mathcal{L}^{-1}(F) = \overline{\mathbf{p}}_0\left\{ \frac{m_i}{\overline{m}} - \sum_{l=1}^{N-1}\frac{\prod\limits_{k}^{N}\left(\omega_k^2 - \omega_{Ql}^2\right)}{(\omega_i^2 - \omega_{Ql}^2)\prod\limits_{k\neq l}^{N-1}\left(\omega_{Qk}^2 - \omega_{Ql}^2\right)}\frac{\cos(\omega_{Ql}t)}{\omega_{Ql}^2} \right\}.$$

The third form is $F = \frac{\hat{A}_{1;i}}{\omega^2 + \omega_j^2}$ with two types of solutions depending on i, for $(i \neq j)$:

$$\mathcal{L}^{-1}(F) = \sum_{l=1}^{N-1}\frac{\prod\limits_{k}^{N}\left(\omega_k^2 - \omega_{Ql}^2\right)}{(\omega_i^2 - \omega_{Ql}^2)(\omega_j^2 - \omega_{Ql}^2)\prod\limits_{k\neq l}^{N-1}\left(\omega_{Qk}^2 - \omega_{Ql}^2\right)}\cos(\omega_{Ql}t)$$

and for $(i = j)$, by using the identity $Q(-\omega_i^2) = \frac{1}{N}\sum\limits_{j=1}^{N}\prod\limits_{k\neq j}^{N}\left(\omega_k^2 - \omega_i^2\right) = \frac{1}{N}\prod\limits_{k\neq i}^{N}\left(\omega_k^2 - \omega_i^2\right)$ we obtain:

$$\mathcal{L}^{-1}(F) = \frac{\prod\limits_{k\neq i}^{N}\left(\omega_k^2 - \omega_i^2\right)}{Q(-\omega_i^2)}\cos(\omega_i t) + \sum_{l=1}^{N-1}\frac{\prod\limits_{k}^{N}\left(\omega_k^2 - \omega_{Ql}^2\right)}{(\omega_i^2 - \omega_{Ql}^2)^2\prod\limits_{k\neq l}^{N-1}\left(\omega_{Qk}^2 - \omega_{Ql}^2\right)}\cos(\omega_{Ql}t) =$$

$$= N\cos(\omega_i t) + \sum_{l=1}^{N-1}\frac{\prod\limits_{k}^{N}\left(\omega_k^2 - \omega_{Ql}^2\right)}{(\omega_i^2 - \omega_{Ql}^2)^2\prod\limits_{k\neq l}^{N-1}\left(\omega_{Qk}^2 - \omega_{Ql}^2\right)}\cos(\omega_{Ql}t).$$

And finally $F = \frac{\hat{A}_{0;i}}{\omega^2 + \omega_j^2}$, again with two solutions, for $(i \neq j)$:

$$\mathcal{L}^{-1}(F) = \sum_{l=1}^{N-1}\frac{\prod\limits_{k}^{N}\left(\omega_k^2 - \omega_{Ql}^2\right)}{(\omega_i^2 - \omega_{Ql}^2)(\omega_j^2 - \omega_{Ql}^2)\prod\limits_{k\neq l}^{N-1}\left(\omega_{Qk}^2 - \omega_{Ql}^2\right)}\frac{\sin(\omega_{Ql}t)}{\omega_{Ql}}$$

and for $(i = j)$:

$$\mathcal{L}^{-1}(F) = N\frac{\sin{(\omega_i t)}}{\omega_i} + \sum_{l=1}^{N-1} \frac{\prod\limits_{k}^{N}\left(\omega_k^2 - \omega_{Ql}^2\right)}{(\omega_i^2 - \omega_{Ql}^2)^2 \prod\limits_{k \neq l}^{N-1}\left(\omega_{Qk}^2 - \omega_{Ql}^2\right)} \frac{\sin{(\omega_{Ql} t)}}{\omega_{Ql}}.$$

Let us now write the resulting inverse transform $\mathcal{L}^{-1}(\hat{\mathbf{p}}_i)(t)$, denoting the constant coefficient $K_{il} \equiv \frac{\prod\limits_{k}^{N}(\omega_k^2 - \omega_{Ql}^2)}{(\omega_i^2 - \omega_{Ql}^2)\prod\limits_{k\neq l}^{N-1}\left(\omega_{Qk}^2 - \omega_{Ql}^2\right)}$:

$$\mathbf{p}_i = \mathbf{p}_{0i}\cos{(\omega_i t)} - \frac{\gamma\mathbf{q}_{0i}}{N}\frac{\sin{(\omega_i t)}}{\omega_i} + \overline{\mathbf{p}}_0\left\{\frac{\gamma}{\omega_i^2 N}\frac{1}{\overline{m}} - \sum_{l=1}^{N-1}\frac{K_{il}\cos{(\omega_{Ql}t)}}{\omega_{Ql}^2}\right\} - \mathbf{p}_{0i}\cos{(\omega_i t)}$$

$$+ \frac{\gamma\mathbf{q}_{0i}}{N}\frac{\sin{(\omega_i t)}}{\omega_i} - \frac{1}{N}\sum_{j=1}^{N}\sum_{l=1}^{N-1}\frac{K_{il}}{\omega_j^2 - \omega_{Ql}^2}\left(\mathbf{p}_{0j}\cos{(\omega_{Ql}t)} - \frac{\gamma\mathbf{q}_{0j}}{N}\frac{\sin{(\omega_{Ql}t)}}{\omega_{Ql}}\right)$$

and after subtracting the terms with $\cos{(\omega_i t)}$ and $\sin{(\omega_i t)}$:

$$\mathbf{p}_i = \overline{\mathbf{p}}_0\left[\frac{m_i}{\overline{m}} - \sum_{l=1}^{N-1}\frac{K_{il}\cos{(\omega_{Ql}t)}}{\omega_{Ql}^2}\right] - \sum_{j}^{N}\sum_{l=1}^{N-1}\frac{K_{il}\left(\mathbf{p}_{0j}\cos{(\omega_{Ql}t)} - \frac{\gamma\mathbf{q}_{0j}}{N}\frac{\sin{(\omega_{Ql}t)}}{\omega_{Ql}}\right)}{N\left(\omega_j^2 - \omega_{Ql}^2\right)}.$$

(2.14)

With this results we can calculate the sum $\frac{1}{N}\sum_i \omega_i^2 \mathbf{p}_i$ needed in Equation (2.18). Using the equalities

$$\sum_{j=1}^{N} K_{jl} = Q(-\omega_{Ql}^2) = 0, \qquad\qquad \sum_{j=1}^{N}\omega_j^2 K_{jl} = N\frac{\prod\limits_{k}^{N}\left(\omega_k^2 - \omega_{Ql}^2\right)}{\prod\limits_{k\neq l}^{N-1}\left(\omega_{Qk}^2 - \omega_{Ql}^2\right)},$$

we write:

$$\frac{1}{N}\sum_i \omega_i^2 \mathbf{p}_i = \overline{\mathbf{p}}_0\left[\frac{\gamma}{N\overline{m}} - \sum_{l=1}^{N-1}\frac{\prod\limits_{k}^{N}(\omega_k^2 - \omega_{Ql}^2)}{\prod\limits_{k\neq l}^{N-1}(\omega_{Qk}^2 - \omega_{Ql}^2)}\frac{\cos{(\omega_{Ql}t)}}{\omega_{Ql}^2}\right] -$$

$$- \frac{1}{N}\sum_{j}^{N}\sum_{l=1}^{N-1}\frac{\prod\limits_{k\neq j}^{N}(\omega_k^2 - \omega_{Ql}^2)}{\prod\limits_{k\neq l}^{N-1}(\omega_{Qk}^2 - \omega_{Ql}^2)}\left(\mathbf{p}_{0j}\cos{(\omega_{Ql}t)} - \frac{\gamma}{N}\mathbf{q}_{0j}\frac{\sin{(\omega_{Ql}t)}}{\omega_{Ql}}\right).$$

We can further simplify this result by combining the cosine terms:

$$\sum_{l=1}^{N-1} \frac{\prod\limits_{k \neq j}^{N}(\omega_k^2 - \omega_{Ql}^2)}{\prod\limits_{k \neq l}^{N-1}(\omega_{Qk}^2 - \omega_{Ql}^2)} \left(\frac{\overline{\mathbf{p}}_0}{\omega_{Ql}^2} + \frac{1}{N}\sum_j^N \frac{\mathbf{p}_j}{\omega_j^2 - \omega_{Ql}^2} \right) \cos\left(\omega_{Ql}t\right),$$

where the bracket gives:

$$\frac{\overline{\mathbf{p}}_0}{\omega_{Ql}^2} + \frac{1}{N}\sum_j^N \frac{\mathbf{p}_j(\omega_{Ql}^2 - \omega_j^2 + \omega_j^2)}{(\omega_j^2 - \omega_{Ql}^2)\omega_{Ql}^2} = \frac{1}{N}\sum_j^N \frac{\mathbf{p}_j\omega_j^2}{(\omega_j^2 - \omega_{Ql}^2)\omega_{Ql}^2}.$$

Returning to the notation $\mathbf{p}_i(t) = S_\perp^t \mathbf{p}_i$, $\mathbf{p}_{0i} \equiv \mathbf{p}_i$, denoting the large multiplications $\Pi_{jl} = \frac{\prod\limits_{k \neq j}^{N}(\omega_k^2 - \omega_{Ql}^2)}{\prod\limits_{k \neq l}^{N-1}(\omega_{Qk}^2 - \omega_{Ql}^2)}$ and $\omega_j^2 = \frac{\gamma}{Nm_j}$, we arrive at the random force:

$$S_\perp^t \mathbf{F}_s = \sum_i S_\perp^t \frac{\omega_i^2}{\gamma}\mathbf{p}_i = \frac{\overline{\mathbf{p}}}{\overline{m}} - \frac{1}{N}\sum_j^N \sum_{l=1}^{N-1} \Pi_{jl}\left(\frac{\mathbf{p}_j}{m_j}\frac{\cos\left(\omega_{Ql}t\right)}{\omega_{Ql}^2} - \mathbf{q}_j\frac{\sin\left(\omega_{Ql}t\right)}{\omega_{Ql}} \right) \quad (2.15)$$

and the term in the memory kernel:

$$-K_s(t)\mathbf{s} = \mathcal{P}_s L S_\perp^t \mathbf{F_s} = -\left[\frac{\gamma}{N\overline{m}} - \sum_{l=1}^{N} \frac{\prod\limits_k(\omega_k^2 - \omega_{Ql}^2)}{\omega_{Ql}^2 \prod\limits_{k \neq l}(\omega_{Qk}^2 - \omega_{Ql}^2)} \cos\left(\omega_{Ql}t\right) \right]\mathbf{s}. \quad (2.16)$$

This concludes the tedious intermezzo.

2.1.2   Summary of the Mori-Zwanzig Evolution Equations

The fruit of our labor are the final evolution equations. For the resolved variables $(\mathbf{Q}, \mathbf{P})$ the final equations are:

$$\frac{\partial}{\partial t}S^t\mathbf{Q} = S^t\frac{\mathbf{P}}{M}, \quad (2.17a)$$

$$\frac{\partial}{\partial t}S^t\mathbf{P} = -S^t V'(\mathbf{Q}) - \int_0^t K(u)S^{t-u}\frac{\mathbf{P}}{M}du + \mathbf{F}(t), \quad (2.17b)$$

where $K(s)$ is from the equation for the memory kernel (2.8) and $\mathbf{F}(t)$ is the random force caused by the small particles, which is described by Equation (2.7).

The evolution equations for the resolved variables $(\mathbf{Q}, \mathbf{P}, \mathbf{s})$ are

$$\frac{\partial}{\partial t}S^t\mathbf{Q} = S^t\frac{\mathbf{P}}{M}, \quad (2.18a)$$

$$\frac{\partial}{\partial t}S^t\mathbf{P} = -S^t\left(V'(\mathbf{Q}) - \gamma\mathbf{s} \right), \quad (2.18b)$$

$$\frac{\partial}{\partial t}S^t\mathbf{s} = -S^t\frac{\mathbf{P}}{M} - \int_0^t K_\mathbf{s}(u)S^{t-u}\mathbf{s}du + F_\mathbf{s}(t), \quad (2.18c)$$

where $K_{\mathbf{s}}(u)$ is from Equation (2.16) and $F_{\mathbf{s}}(t)$ is given by Equation (2.15).

Let us compare the two evolutions. The memory kernels are:

$$K(t, u) = K(u)S^{t-u}\frac{\mathbf{P}}{M},$$

$$K_{\mathbf{s}}(t, u) = K_{\mathbf{s}}(u)S^{t-u}\mathbf{s},$$

$$K(u) = \sum_j \frac{\gamma}{N}\cos(\omega_j u),$$

$$K_{\mathbf{s}}(u) = \frac{\gamma}{N\overline{m}} - \sum_{l=1}^{N}\frac{\prod_k (\omega_k^2 - \omega_{Ql}^2)}{\omega_{Ql}^2 \prod_{k \neq l}(\omega_{Qk}^2 - \omega_{Ql}^2)}\cos(\omega_{Ql}t),$$

and the random forces are

$$F(t) = \sum_{j=1}^{N}\frac{\gamma}{N}\left[(\mathbf{q_j} - \mathbf{Q})\cos(\omega_j t) + \frac{\mathbf{p}_j}{\omega_j m_i}\sin(\omega_j t)\right],$$

$$F_{\mathbf{s}}(t) = \frac{\overline{\mathbf{p}}}{m} - \frac{1}{N}\sum_{j=1}^{N}\sum_{l=1}^{N-1}\frac{\prod_{k \neq j}^{N}(\omega_k^2 - \omega_{Ql}^2)}{\prod_{k \neq l}^{N-1}(\omega_{Qk}^2 - \omega_{Ql}^2)}\left(\frac{\mathbf{p}_j}{m_j}\frac{\cos(\omega_{Ql}t)}{\omega_{Ql}^2} - \mathbf{q}_j\frac{\sin(\omega_{Ql}t)}{\omega_{Ql}}\right).$$

Equation (2.17a) and (2.18a) are the same. However, random force and memory kernel are in one case in the evolution of $\mathbf{P}$ (2.17b), whereas in the other in the evolution of the additional variable $\mathbf{s}$ (2.18c). The structure of these terms is then similar, with a difference in frequencies and additional constant term in $K_{\mathbf{s}}$ and $F_{\mathbf{s}}$.

2.1.3 Limit for $N \to \infty$

Our approach tried to find a differential form through a choice of variables $(\mathbf{Q}, \mathbf{P}, \mathbf{s})$. This choice was motivated by a different approach shown in [16], wherein a limit of Equation (2.17) for $N \to \infty$ is computed in the case of a Cauchy distribution of the frequencies ω_i. In this limit, the equations can be formulated as a set of stochastic differential equations from [16]. We will make a quick review of the derivation of the stochastic equations. Detailed computation is done in [16, 17].

Rewriting the equations from (2.17) in a form of a second order ODE:

$$\ddot{\mathbf{Q}} + V'(\mathbf{Q}) + \int_0^t K(t - u)\dot{\mathbf{Q}}(u)\mathrm{d}u = F(t), \tag{2.20}$$

with $K(t - u)$ and $F(t)$ from (2.17b) (i.e. $K(t) = \sum_j \frac{\gamma}{N}\cos(\omega_j t)$,

$F(t) = \sum_j \frac{\gamma}{N}\left[(\mathbf{q}_j - \mathbf{Q})\cos(\omega_j t) + \frac{\mathbf{p}_j}{\omega_j m_j}\sin(\omega_j t)\right]$).

The goal is to find the limit of N going to infinity. This limit is heavily dependent on the distribution of the frequencies ω_i. There are previous works done for

both random distributions [18, 19, 16, 17] as well as deterministic distribution of frequencies, which leads to solutions relying on Fourier series [20]. Here we have specific outcome in mind and will therefore further follow [16] with the choice of frequency distribution:

$$p(\omega) = \begin{cases} \frac{2\omega_*}{\pi} \frac{1}{\omega_*^2 + \omega^2} & \text{if } \omega \geq 0 \\ 0 & \text{otherwise} \end{cases}, \quad (2.21)$$

for which the limit of the memory kernel is (using the strong law of large numbers):

$$\lim_{N \to \infty} \sum_j \frac{\gamma}{N} \cos(\omega_j t) = \gamma \lim_{N \to \infty} \frac{1}{N} \sum_j \cos(\omega_j t) = \gamma \langle \cos(\omega t) \rangle =$$

$$= \gamma \int_0^\infty \frac{2\omega_*}{\pi} \frac{\cos(\omega t)}{\omega_*^2 + \omega^2} d\omega = \gamma e^{-|t\omega_*|}.$$

To find the limit of the force on the right hand side, we will first focus on the initial distributions of $\mathbf{p}_i$ and $\mathbf{q}_i$. The values are pulled from a canonical distribution with the Hamiltonian (2.1), thus initial conditions for each $\mathbf{p}_i$ and $\mathbf{q}_i$ is independent and Gaussian. For $\mathbf{p}_i$ the Gaussian has the mean 0 and the variance $\frac{m_i}{\beta}$ and for $\mathbf{q}_i$ the mean is $\mathbf{Q}$ and the variance $\frac{N}{\gamma\beta}$. We will transition to random variables h_i, g_i with zero mean and unit variance:

$$\mathbf{h}_i = \sqrt{\frac{\beta}{m_i}} \mathbf{p}_i, \qquad \mathbf{g}_i = \sqrt{\frac{\beta\gamma}{N}} (\mathbf{q}_i - \mathbf{Q}),$$

$$F(t) = \sqrt{\frac{\gamma}{N\beta}} \sum_j \left[\mathbf{g}_j \cos(\omega_j t) + \mathbf{h}_j \sin(\omega_j t) \right].$$

In [17], it is shown that in the limit $N \to \infty$, $\xi(t) \equiv \sqrt{\beta}F(t)$ is a Gaussian process with zero mean and covariance:

$$\langle \xi(t)\xi(t') \rangle = \gamma \int_0^\infty p(\omega) \cos(\omega(t - t')) d\omega = K(t - t') = \gamma e^{-|(t-t')\omega_*|}.$$

With this knowledge, we may observe that the force is a stationary Ornstein-Uhlenbeck process (dW_t is a "differential" of the Wiener process):

$$d\xi = -\omega_* \xi dt + \sqrt{2\gamma\omega_*} dW_t$$

and thanks to the exponential kernel we may rewrite Equation (2.20):

$$\ddot{\mathbf{Q}} + V'(\mathbf{Q}) + \int_0^t K(t - u)\dot{\mathbf{Q}}(u)du = F(t)$$

$$\ddot{\mathbf{Q}} + V'(\mathbf{Q}) + \int_0^t \gamma e^{-(t-u)\omega_*}\dot{\mathbf{Q}}(u)du = \frac{1}{\sqrt{\beta}}\xi,$$

$$\ddot{\mathbf{Q}} + V'(\mathbf{Q}) - \gamma\mathbf{s} = 0,$$

with

$$\mathbf{s} = -\int_0^t e^{-\omega_*(t-\tau)}\dot{\mathbf{Q}}(\tau)\mathrm{d}\tau + \frac{1}{\gamma\sqrt{\beta}}\xi$$

and for differential of $\mathbf{s}$ we will use the equation for $d\xi$:

$$d\mathbf{s} = -\dot{\mathbf{Q}}(t) + \omega_*\int_0^t e^{-\omega_*(t-\tau)}\frac{\mathbf{P}(\tau)}{M}\mathrm{d}\tau + \frac{1}{\gamma\sqrt{\beta}}d\xi =$$

$$= -\dot{\mathbf{Q}} + \omega_*\left(\int_0^t e^{-\omega_*(t-\tau)}\frac{\mathbf{P}(\tau)}{M}\mathrm{d}\tau - \frac{1}{\gamma\sqrt{\beta}}\xi\mathrm{d}t\right) + \sqrt{\frac{2\omega_*}{\gamma\beta}}\mathrm{d}W_t$$

$$d\mathbf{s} = -\dot{\mathbf{Q}} - \omega_*\mathbf{s} + \sqrt{\frac{2\omega_*}{\gamma\beta}}\mathrm{d}W_t.$$

This in turn means that we can write the evolution as a system of stochastic differential equations in the Ito sense:

$$\dot{\mathbf{Q}} = \frac{\mathbf{P}}{M}, \tag{2.22a}$$

$$\dot{\mathbf{P}} = -V'(\mathbf{Q}) + \gamma\mathbf{s}, \tag{2.22b}$$

$$\dot{\mathbf{s}} = -\frac{\mathbf{P}}{M} - \omega_*\mathbf{s} + \sqrt{\frac{2\omega_*}{\beta\gamma}}\dot{W} \tag{2.22c}$$

with initial conditions denoting $(\mathbf{Q}_0, \mathbf{P}_0, \mathbf{s}_0 = \frac{1}{\gamma\sqrt{\beta}}\xi_0)$. Unlike in the original paper, here we are using a general frequency parameter ω_*. The similarity of Equation (2.22) to Equation (2.18) motivates us to focus in the following section on the resolved variables (Q, P, s).

2.2   The Lack-of-fit Reduction

We will follow the steps outlined in Section 1.3.2. For simplicity, the Kac-Zwanzig model will be in one dimension and the potential $V(Q)$ will be harmonic, i.e. $V(Q) = \frac{\alpha Q^2}{2}$.

The **first step** is formulating the upper evolution (from Equation (1.14)). The detailed evolution is reversible and as such has zero dissipation potential $^\uparrow\Xi$. However, we will need to maximise the upper entropy of the system $^\uparrow S$. This leads us to abandon the exact canonical description, used in the previous section, and instead use normalised distribution functions f as our upper variables. The distribution functions have continuous parameters $Q, P, q_1, p_1, ...q_N, p_N$, i.e. positions and momenta of (N+1) particles. The microscopic evolution is found using the Liouville equation:

$$\frac{\partial f}{\partial t} = \{f, E\}^{(f)} = N! \sum_{i=0}^{N} \left[\frac{\partial f}{\partial p_i} \frac{\partial E_f}{\partial q_i} - \frac{\partial f}{\partial q_i} \frac{\partial E_f}{\partial p_i} \right], \tag{2.23}$$

where $q_0 = Q, p_0 = P$ and $E_f = \frac{\delta E}{\delta f}$. This evolution corresponds to the Poisson bivector, which acts on A, B as functions of the distribution f:

$$\{A, B\}^{(f)} = N! \int \dots \int \mathrm{d}Q\mathrm{d}P\mathrm{d}[\mathbf{i}] f \sum_{i=0}^{N} \left[\frac{\partial}{\partial q_i} \left(\frac{\delta A}{\delta f} \right) \frac{\partial}{\partial p_i} \left(\frac{\delta B}{\delta f} \right) - \right.$$
$$\left. - \frac{\partial}{\partial q_i} \left(\frac{\delta B}{\delta f} \right) \frac{\partial}{\partial p_i} \left(\frac{\delta A}{\delta f} \right) \right]. \tag{2.24}$$

The microscopic entropy has the form:

$$^{\uparrow}S = -\frac{k_B}{N!} \int \int \dots \int f \ln \left(h^{(N+1)} f \right) \mathrm{d}Q\mathrm{d}P\mathrm{d}[\mathbf{i}] \tag{2.25}$$

and the total energy of the system is

$$^{\uparrow}E(f) = E(f) = \frac{1}{N!} \int \int \dots \int f e \, \mathrm{d}Q\mathrm{d}P\mathrm{d}[\mathbf{i}], \tag{2.26}$$

where $e = \frac{1}{2M} P^2 + \frac{\alpha Q^2}{2} + \sum_{i=1}^{N} \left[\frac{p_i^2}{2m_i} + \frac{\gamma}{2N} (q_i - Q)^2 \right]$.

The **second step** is the formulation of the lower variables, i.e. the projection on the lower variables. The macroscopic variables will be (Q, P, s), as was the second case in the previous section. Since the microscopic description are the distribution functions, our projection will be the mean values:

$$\overline{Q}(f) = \frac{1}{N!} \int \int \dots \int f Q \, \mathrm{d}Q\mathrm{d}P\mathrm{d}[\mathbf{i}], \tag{2.27a}$$

$$\overline{P}(f) = \frac{1}{N!} \int \int \dots \int f P \, \mathrm{d}Q\mathrm{d}P\mathrm{d}[\mathbf{i}], \tag{2.27b}$$

$$\overline{s}(f) = \frac{1}{N!} \int \int \dots \int f \left(\frac{1}{N} \sum_{i=1}^{N} q_i - Q \right) \mathrm{d}Q\mathrm{d}P\mathrm{d}[\mathbf{i}]. \tag{2.27c}$$

Above that we need to control the temperature of the system and therefore the fourth variable will be the energy of the system E. Together we write the lower variables $\mathbf{y} = (\overline{Q}, \overline{P}, \overline{s}, E)$.

The **third step** is the static reduction, i.e. entropy $^{\uparrow}S$ is maximised with constrains corresponding to the lower variables $(\overline{Q}, \overline{P}, \overline{s}, E)$ and also to the normalisation of the distribution function:

$$\frac{\delta}{\delta f} \left[-^{\uparrow}S(f) + \overline{Q}Q^* + \overline{P}P^* + \overline{s}s^* + EE^* + \nu^* \cdot 1 \right] = 0. \tag{2.28}$$

The functional derivatives are calculated from the defining equations (2.27), (2.25) and (2.26):

$$\frac{\delta \overline{Q}}{\delta f} = \frac{Q}{N!}, \qquad \frac{\delta \overline{P}}{\delta f} = \frac{P}{N!}, \qquad \frac{\delta \overline{s}}{\delta f} = \frac{s}{N!}, \tag{2.29}$$

$$\frac{\delta^\uparrow S}{\delta f} = -\frac{k_B}{N!} \left(\ln\left(h^{(N+1)} f\right) + 1 \right), \qquad \frac{\delta^\uparrow E}{\delta f} = \frac{e}{N!}. \tag{2.30}$$

The extremal distribution is calculated as:

$$\tilde{f} = \frac{1}{h^{N+1}} \exp\left(-\frac{\nu^*}{k_B} - 1\right) \exp\left(-\frac{QQ^*}{k_B}\right) \exp\left(-\frac{PP^*}{k_B}\right) \exp\left(-\frac{ss^*}{k_B}\right) \exp\left(-\frac{eE^*}{k_B}\right). \tag{2.31}$$

The conjugate variables are $(Q^*, P^*, s^*, E^*, \nu^*)$. Before further calculations of the conjugate variables as functions of the desired macroscopic evolution, we will determine the normalisation $\nu^*(Q^*, P^*, s^*, E^*)$:

$$\frac{I}{N!} \equiv \frac{1}{N!} \int dQ \int dP \int dq_1 \int dp_1 ... \int d\mathbf{q}_N \int d\mathbf{p}_N \tilde{f} \overset{!}{=} 1.$$

The integral I can be calculated in two parts, first for the momenta and second for the positions. The integral over the space of momenta is:

$$\int dP e^{-\frac{1}{2k_B}\left(E^*\frac{P^2}{M} + 2PP^*\right)} \prod_{i=1}^{N} \int dp_i e^{-\frac{E^*}{k_B}\frac{p_i^2}{2m_i}} = \left(\frac{2\pi k_B}{E^*}\right)^{\frac{N+1}{2}} \sqrt{M} \left[\prod_i \sqrt{m_i}\right] e^{\frac{M(\mathbf{P}^*)^2}{2k_B E^*}},$$

which is calculated using the Gaussian integration. The integral over positions is calculated as multivariate normal distribution, i.e. Gaussian integration for matrices:

$$I_{Qq_i} = \int dQ \int d[q_i] e^{-\frac{E^*}{2k_B}\left(2\mathbf{q}^T \cdot \mathbf{b} + \mathbf{q}^T \tilde{A}\mathbf{q}\right)} = \int dQ \int d[q_i] e^{-\frac{1}{2}\left(2\sqrt{\frac{E^*}{k_B}}\mathbf{q}^T \cdot \mathbf{b} + \mathbf{q}^T A\mathbf{q}\right)},$$

$$A = \begin{pmatrix} (\alpha + \gamma) & -\frac{\gamma}{N} & \cdots \\ -\frac{\gamma}{N} & \frac{\gamma}{N}\mathbb{I} & \\ \cdots & & \end{pmatrix}, \mathbf{b} = \left(\frac{Q^* - s^*}{E^*}, \quad \frac{s^*}{E^*N} \quad \cdots \right),$$

where A is the inverse of the covariance matrix and with $\mathbf{b}$ we would calculate the mean values. Finally we write

$$I_{Qq_i} = \left(\frac{2\pi k_B}{E^*}\right)^{\frac{N+1}{2}} \frac{e^{-\frac{E^*}{2k_B}\mathbf{b}^T A^{-1}\mathbf{b}}}{\sqrt{\det A}} = \left(\frac{2\pi k_B}{E^*}\right)^{\frac{N+1}{2}} \frac{1}{\sqrt{\alpha}} \left[\prod_i \sqrt{\frac{N}{\gamma}}\right] e^{\frac{(\mathbf{Q}^*)^2}{\alpha} + \frac{(s^*)^2}{\gamma}}{2k_B E^*}.$$

Putting the calculations together gives:

$$\frac{I}{N!} = \frac{e^{-\frac{\nu^*}{k_B} - 1}}{h^{N+1}N!} \left(\frac{2\pi k_B}{E^*}\right)^{N+1} \sqrt{\frac{M}{\alpha}} \left[\prod_i \sqrt{\frac{m_i N}{\gamma}}\right] \exp \frac{\frac{(\mathbf{Q}^*)^2}{\alpha} + \frac{(s^*)^2}{\gamma} + M(\mathbf{P}^*)^2}{2k_B E^*} \overset{!}{=} 1$$

and as a result we write the normalisation:

$$\nu^*(\mathbf{y}^*) = \frac{\Sigma}{E^*} - (N+1)k_B \ln\left(\frac{E^*\hbar}{k_B}\right) - k_B \ln(N!) - k_B +$$

$$+ \frac{k_B}{2} \ln\left(\frac{M}{\alpha}\right) + \frac{k_B}{2} \sum_{i=1}^{N} \ln\left(\frac{m_i N}{\gamma}\right),$$

where $\mathbf{y}^* = (Q^*, P^*, s^*, E^*)$ will be from now on the vector of the conjugate lower variables. We denote for brevity

$$\Sigma = \frac{(\mathbf{Q}^*)^2}{2\alpha} + \frac{(\mathbf{s}^*)^2}{2\gamma} + \frac{M(\mathbf{P}^*)^2}{2}. \tag{2.32}$$

From Equation (2.27) and (2.26), we will find the conjugate variables as functions of the resolved variables $\mathbf{y} = (\overline{Q}, \overline{P}, \overline{s}, E)$. A useful observation is

$$\mathbf{y}^i = -\frac{k_B}{N!} \frac{\partial I}{\partial \mathbf{y}^*_i}\bigg|_{\nu^*=const.},$$

from which we get the functions $\mathbf{y}(\mathbf{y}^*)$:

$$\mathbf{y} = \left(-\frac{Q^*}{\alpha E^*}, -\frac{MP^*}{E^*}, -\frac{s^*}{\gamma E^*}, \frac{1}{E^*}\left(k_B(N+1) + \frac{\Sigma}{E^*}\right)\right), \tag{2.33}$$

as well as the conjugate variables $\mathbf{y}^*(\mathbf{y})$:

$$\mathbf{y}^* = \left(-\alpha\overline{Q}E^*, -\frac{\overline{P}}{M}E^*, -\gamma\overline{s}E^*, \frac{k_B(N+1)}{U}\right), \tag{2.34}$$

where $U = E - \frac{1}{2}\left(\alpha\overline{Q}^2 + \frac{\overline{P}^2}{M} + \gamma\overline{s}^2\right)$.

From Equation 2.28 we get the entropy $^{\downarrow}S^*(\mathbf{y}^*)$ and by a full Legendre transform we arrive at the lower entropy:

$$^{\downarrow}S(\mathbf{y}) = k_B(N+1)\ln\frac{U}{\hbar} + S_0, \tag{2.35}$$

with the constant S_0 given by:

$$S_0 = k_B\left(\frac{1}{2}\left[\ln\left(\frac{M}{\alpha}\right) - \sum_{i=1}^{N}\ln\left(\frac{m_i N}{\gamma}\right)\right] - \ln N! - (N+1)(\ln(N+1) - 1)\right).$$

The **fourth step** is the calculation of the apparent lower-level energy from Equation (2.56), calculated as $^{\uparrow}E(f(\mathbf{y}^*(\mathbf{y}(f))))$:

$$^{\uparrow}\overline{E}(f) = \frac{1}{2}\left(\alpha\overline{Q}^2(f) + \frac{\overline{P}^2(f)}{M} + \gamma\overline{s}^2(f)\right) + \hbar\exp\frac{^{\downarrow}S(\mathbf{y}(f)) - S_0}{k_B(N+1)}. \tag{2.36}$$

In **step five**, the residuum (defined in Equation (2.39)) will introduce $\dot{\mathbf{y}}^* = (\dot{Q}^*, \dot{P}^*, \dot{s}^*, \dot{E}^*)$ as our new variables. The residuum also parametrically depends on (Q, P, q_i, p_i) vie the maximal distribution $\tilde{f}$:

$$R = \left\{\tilde{f}, ^{\uparrow}\overline{E}\right\}^{(f)} - \frac{\partial \tilde{f}}{\partial \mathbf{y}_a^*}\dot{\mathbf{y}}_a^*.$$

We will use the Liouville equation (2.23) for the first term $\left\{f, ^{\uparrow}\overline{E}\right\}^{(f)}$:

$$\frac{\delta^{\uparrow}\overline{E}}{\delta f} = -Q^*\frac{Q}{E^*N!} - P^*\frac{P}{E^*N!} - s^*\frac{s}{E^*N!} + \hbar\frac{e^{\frac{\downarrow S(\mathbf{y}(f))-S_0}{k_B(N+1)}}}{k_B(N+1)}\frac{\delta^{\downarrow}S(\mathbf{y}(f))}{\delta f}.$$

For convenience, we denote $\spadesuit \equiv \hbar\exp\frac{\downarrow S(\mathbf{y}(f))-S_0}{k_B(N+1)}$ and from the MaxEnt equation (2.28) we have

$$\frac{\delta^{\downarrow}S(\mathbf{y}(f))}{\delta f} = \frac{1}{N!}\left(eE^* + QQ^* + PP^* + ss^*\right).$$

The necessary derivatives are:

$$-\frac{\partial \tilde{f}}{\partial Q} = \frac{\tilde{f}\left[Q^* - s^* + \frac{\partial e}{\partial Q}E^*\right]}{k_B}, \qquad \frac{\partial^{\uparrow}\overline{E}_f}{\partial P} = \frac{1}{N!}\left(-\frac{P^*}{E^*} + \spadesuit\left(P^* + E^*\frac{\partial e}{\partial P}\right)\right),$$

$$\frac{\partial \tilde{f}}{\partial P} = -\frac{\tilde{f}}{k_B}\left[P^* + \frac{\partial e}{\partial P}E^*\right], \qquad \frac{\partial^{\uparrow}\overline{E}_f}{\partial Q} = \frac{1}{N!}\left(\frac{s^* - Q^*}{E^*} + \right.$$

$$\left. + \spadesuit\left(Q^* - s^* + E^*\frac{\partial e}{\partial Q}\right)\right),$$

$$-\frac{\partial \tilde{f}}{\partial q_i} = \frac{\tilde{f}}{k_B}\left[\frac{s^*}{N} + \frac{\partial e}{\partial q_i}E^*\right], \qquad \frac{\partial^{\uparrow}\overline{E}_f}{\partial p_i} = \frac{\spadesuit}{N!}\frac{\partial e}{\partial p_i}E^*,$$

$$\frac{\partial \tilde{f}}{\partial p_i} = -\frac{E^*}{k_B}\frac{\partial e}{\partial p_i}\tilde{f}, \qquad \frac{\partial^{\uparrow}\overline{E}_f}{\partial q_i} = \frac{1}{N!}\left(\frac{s^*}{N} + \spadesuit\frac{\partial e}{\partial q_i}E^*\right).$$

The second term $\frac{\partial f}{\partial \mathbf{y}_a^*}\dot{\mathbf{y}}_a^*$ requires further derivatives:

$$\frac{\partial \tilde{f}}{\partial Q^*} = -\frac{\tilde{f}}{k_B}\left(Q + \frac{Q^*}{E^*\alpha}\right),$$

$$\frac{\partial \tilde{f}}{\partial P^*} = -\frac{\tilde{f}}{k_B}\left(P + \frac{MP^*}{E^*}\right),$$

$$\frac{\partial \tilde{f}}{\partial s^*} = -\frac{\tilde{f}}{k_B}\left(s + \frac{s^*}{E^*\gamma}\right),$$

$$\frac{\partial \tilde{f}}{\partial E^*} = -\frac{\tilde{f}}{k_B}\left(E - \frac{1}{E^*}\left(\frac{\Sigma}{E^*} + k_B(N+1)\right)\right).$$

Thus we arrive at the residuum:

$$R = \frac{f}{k_B}\left[(\mathbf{y}^{*T}, \dot{\mathbf{y}}^{*T})\mathbf{V} - \dot{\mathbf{y}}^{*T}\mathbf{y}(\mathbf{y}^*)\right], \tag{2.39}$$

where the dependence on the parameters (Q, P, q_i, p_i) is only in the vector $\mathbf{V}$:

$$\mathbf{V}^T = \left(\frac{P}{M}, \gamma s - \alpha Q, -\frac{P}{M} + \frac{1}{N}\sum_i \frac{p_i}{m_i}, 0, Q, P, s, e\right).$$

In **step six** Lagrangian is calculated from the defining equation (1.17) using the residuum (2.39):

$$\mathcal{L} = -\frac{1}{2}\int d\mathbf{Q}' \int d\mathbf{Q} \int d\mathbf{P}' \int d\mathbf{P} ... \int d\mathbf{p}_N' \int d\mathbf{p}_N R(f') \frac{\delta^2(^\uparrow S)}{\delta f' \delta f} R(f).$$

The summation over discrete indices in Equation (1.17) is replaced by integration over the parametric space of f. Using Equation (2.30), the Hessian of the upper entropy is:

$$\frac{\delta^2(^\uparrow S)}{\delta f' \delta f} = -\frac{k_B}{N!}\frac{1}{f}\delta(Q - Q')\delta(P - P')\delta(1 - 1')...\delta(N - N').$$

The Dirac functions will cancel out half of the integrals and the rest will result in mean values $\langle \cdot \rangle$, arriving at the Lagrangian:

$$\mathcal{L} = \frac{1}{2}(\mathbf{y}^{*T}, \dot{\mathbf{y}}^{*T})\begin{pmatrix} \mathbb{A} & \mathbb{B} \\ \mathbb{B}^T & \mathbb{C} \end{pmatrix}\begin{pmatrix} \mathbf{y}^* \\ \dot{\mathbf{y}}^* \end{pmatrix}, \quad \mathbb{A} = \mathbb{A}^T \in \mathbb{R}^{4\times4}, \quad \mathbb{B} \in \mathbb{R}^{4\times4}, \quad \mathbb{C} = \mathbb{C}^T \in \mathbb{R}^{4\times4}.$$

(2.40)

The matrices $\mathbb{A}, \mathbb{B}$ and $\mathbb{C}$ are:

$$\mathbb{A} = \frac{1}{E^*}\begin{pmatrix} \frac{1}{M} & 0 & -\frac{1}{M} & 0 \\ 0 & \alpha + \gamma & 0 & 0 \\ -\frac{1}{M} & 0 & \frac{1}{M} + \frac{\overline{\omega^2}}{\gamma} & 0 \\ 0 & 0 & 0 & 0 \end{pmatrix},$$

(2.41)

where $\overline{\omega^2} = \frac{1}{N}\sum_i \omega_i^2$,

$$\mathbb{B} = \frac{1}{E^*}\begin{pmatrix} 0 & 1 & 0 & -\frac{P^*}{E^*} \\ -1 & 0 & 1 & \frac{Q^* - s^*}{E^*} \\ 0 & -1 & 0 & \frac{P^*}{E^*} \\ 0 & 0 & 0 & 0 \end{pmatrix},$$

(2.42)

$$\mathbb{C} = \frac{1}{E^*}\begin{pmatrix} \frac{1}{\alpha} & 0 & 0 & -\frac{Q^*}{E^*\alpha} \\ 0 & M & 0 & -\frac{MP^*}{E^*} \\ 0 & 0 & \frac{1}{\gamma} & -\frac{s^*}{E^*\gamma} \\ -\frac{Q^*}{E^*\alpha} & -\frac{MP^*}{E^*} & -\frac{s^*}{E^*\gamma} & \frac{k_B E^*(N+1) + 2\Sigma}{(E^*)^2} \end{pmatrix}$$

(2.43)

with Σ from Equation 2.32.

Step seven is computing the Legendre transform of the Lagrangian:

$$\mathcal{H} = -\mathcal{L} + z^a \dot{\mathbf{y}}^*_a(\mathbf{y}^*, \mathbf{z}),$$

(2.44)

where $\mathbf{z}^a = -\frac{\partial \psi}{\partial \mathbf{y}_a^*} = \frac{\partial \mathcal{L}}{\partial \dot{\mathbf{y}}^*_a}$. The inverse transformation $\dot{\mathbf{y}}^*(\mathbf{y}^*, \mathbf{z})$ is found from:

$$\mathbf{z} = \mathbb{B}^T \mathbf{y}^* + \mathbb{C}\dot{\mathbf{y}}^*$$

and therefore is:

$$\dot{\mathbf{y}}^* = \mathbb{C}^{-1}\left(\mathbf{z} - \mathbb{B}^T\mathbf{y}^*\right). \tag{2.45}$$

From calculations, we get the inverse matrix $\mathbb{C}^{-1}$:

$$\mathbb{C}^{-1} = E^*\mathrm{diag}\left(\alpha, \quad \tfrac{1}{M}, \quad \gamma, \quad 0\right) + \frac{1}{k_B(N+1)}\begin{pmatrix} Q^* \\ P^* \\ s^* \\ E^* \end{pmatrix}\begin{pmatrix} Q^*, & P^*, & s^*, & E^* \end{pmatrix}. \tag{2.46}$$

The **eight step** is formulating and solving the Hamilton-Jacobi equation for ψ in the form given by Equation (1.19). Placing $\mathcal{H} = 0$ and $\mathbf{z} \equiv -\frac{\partial \psi}{\partial \mathbf{y}^*}$ leads to the key partial differential equation and since $\mathbb{C}^{-1} = (\mathbb{C}^{-1})^T$, we can write:

$$0 = \frac{1}{2}\left[-\mathbf{y}^{*T}\mathbb{A}\mathbf{y}^* + \left(\frac{\partial \psi}{\partial \mathbf{y}^*}^T + \mathbf{y}^{*T}\mathbb{B}\right)\mathbb{C}^{-1}\left(\frac{\partial \psi}{\partial \mathbf{y}^*} + \mathbb{B}^T\mathbf{y}^*\right)\right]. \tag{2.47}$$

Few simplifications will be made in order to solve this equation:

The first simplification is that E^*, as an inverse temperature, is constant (we are working in an isothermal system) and we will neglect the dependence of ψ on E^*. Therefore, instead of E^* we will write from now on $\frac{1}{T}$ and replace four by four matrices by matrices three by three, crossing out the fourth column and row. The second simplification is the negligence of higher orders of the conjugate variables Q^*, P^* and s^*. Combining the two simplifications gives the matrices $\mathbb{A}, \mathbb{B}$ and $\mathbb{C}^{-1}$ in the form:

$$\mathbb{A} = T\begin{pmatrix} \frac{1}{M} & 0 & -\frac{1}{M} \\ 0 & \alpha+\gamma & 0 \\ -\frac{1}{M} & 0 & \frac{1}{M}+\frac{\overline{\omega^2}}{\gamma} \end{pmatrix}, \quad \mathbb{B} = T\begin{pmatrix} 0 & 1 & 0 \\ -1 & 0 & 1 \\ 0 & -1 & 0 \end{pmatrix} \quad \mathbb{C}^{-1} = \frac{1}{T}\begin{pmatrix} \alpha & 0 & 0 \\ 0 & \frac{1}{M} & 0 \\ 0 & 0 & \gamma \end{pmatrix}.$$

The third simplification is taking a near-equilibrium system, for which $\psi = \frac{T}{2}\mathbf{y}^{*T}\mathbb{M}\mathbf{y}^*$ with $\mathbb{M}$ being a symmetric three by three matrix.

Derivative of the dissipation potential is $\frac{\partial \psi}{\partial \mathbf{y}^*} = T\mathbb{M}\mathbf{y}^*$ and the Hamilton-Jacobi partial differential equation is now a set of algebraic equations:

$$\mathbf{y}^{*T}\mathbb{A}\mathbf{y}^* = \left(\mathbf{y}^{*T}\mathbb{B} + T\mathbf{y}^{*T}\mathbb{M}\right)\mathbb{C}^{-1}\left(\mathbb{B}^T\mathbf{y}^* + T\mathbb{M}\mathbf{y}^*\right)$$

and after multiplying the matrices, we arrive at:

$$-\mathbb{M}\mathbb{C}^{-1}\mathbb{M} - \mathbb{M}\mathbb{C}^{-1}\mathbb{B}^T - \mathbb{B}\mathbb{C}^{-1}\mathbb{M} + \mathbb{A} - \mathbb{B}\mathbb{C}^{-1}\mathbb{B}^T = 0, \tag{2.48}$$

where matrices are written without the coefficient T. Equation (2.47) then becomes a set of 6 equations for 6 unknown elements of the matrix $\mathbb{M}$. Thus we have is the regulator problem of a Riccati equation. We can readily use theorems

about existence and uniqueness of solutions from [12], outlined in Section 1.3.1. Since we are describing a dissipative solution, the matrix needs to be convex (the property written in equation (1.10)). This solution is then called *stabilising solution.* The theorems build on the properties of matrices $\mathbb{C}^{-1}\mathbb{B}^T$:

$$\mathbb{C}^{-1}\mathbb{B}^T = \begin{pmatrix} 0 & -\alpha & 0 \\ \frac{1}{M} & 0 & -\frac{1}{M} \\ 0 & \gamma & 0 \end{pmatrix}$$

$\mathbb{G} \equiv \left(\mathbb{A} - \mathbb{B}\mathbb{C}^{-1}\mathbb{B}^T \right)$:

$$\mathbb{G} = \begin{pmatrix} 0 & 0 & 0 \\ 0 & 0 & 0 \\ 0 & 0 & \frac{\omega^2}{\gamma} \end{pmatrix}$$

and $\mathbb{C}^{-1}$. In the theorems from Subsection 1.3.1, the matrices $\mathbb{G}$ and $\mathbb{C}^{-1}$ are in the form of a multiplication between some matrix and its transpose. However, both $\mathbb{G}$ and $\mathbb{C}^{-1}$ are diagonal and thus this split is a trivial square root of the diagonal terms and so we can use in the theorems the original forms $\mathbb{G}$ and $\mathbb{C}^{-1}$ instead of the square root.

In Theorem 1, the necessary and sufficient condition for existence of the stabilising solution is that the pair $(\mathbb{C}^{-1}\mathbb{B}^T, \mathbb{C}^{-1})$ is stabilizable (Definition 2) and $Re\lambda \neq 0$ for all eigenvalues λ of $\mathbb{M}$. The first condition holds since $\mathbb{C}^{-1}$ is diagonal and finding the matrix L from the theorem, i.e. such that non diagonal elements are zero and diagonal is negative, is trivial.

In Theorem 2 the necessary and sufficient condition for uniqueness of such solution is that the pair $(\mathbb{G}, \mathbb{C}^{-1}\mathbb{B}^T)$ is detectable (Definition 3). For that we need to find the eigenvalues of $\mathbb{C}^{-1}\mathbb{B}^T$:

$$\mathbb{C}^{-1}\mathbb{B}^T = \begin{pmatrix} 0 & -\alpha & 0 \\ \frac{1}{M} & 0 & -\frac{1}{M} \\ 0 & \gamma & 0 \end{pmatrix}, \lambda_0 = 0, \lambda_\pm = \pm i\sqrt{\frac{\alpha+\gamma}{M}}, \mathbf{v}_0 = \begin{pmatrix} 1 \\ 0 \\ 1 \end{pmatrix}, \mathbf{v}_\pm = \begin{pmatrix} -\alpha \\ \pm i\sqrt{\frac{\alpha+\gamma}{M}} \\ \gamma \end{pmatrix}.$$

None of the eigenvectors lies within the kernel of the matrix $\mathbb{G}$ and thus the Theorem 2 holds.

With this knowledge, we may find the nonnegative real solution of the equations. First, we will make an ansatz inspired by the results a numerical calculation done using the programming language Julia, using the package MatrixEquations.jl [21]. Let us approximate the values of the matrix elements $m_{13} \approx \tilde{m}_{13}, m_{23} = -1 + \tilde{m}_{23}$, so that $\tilde{m}_{13}^2 \approx 0$, $\tilde{m}_{23}^2 \approx 0$ and $\tilde{m}_{23}\tilde{m}_{13} \approx 0$. The tilde denotes small perturbations from the approximate value. This leads to the decoupling of the six equations (2.48) to two sets with three equations each. The first set is for the matrix elements m_{11}, m_{12} and m_{22}:

$$\alpha m_{11}^2 + \frac{1}{M}m_{12}^2 + \frac{2m_{12}}{M} = 0,$$

$$\alpha m_{12}^2 + \frac{1}{M}m_{22}^2 - 2\alpha m_{12} + \gamma = 0,$$

$$\alpha m_{11} m_{12} + \frac{1}{M} m_{12} m_{22} - \alpha m_{11} + \frac{m_{22}}{M} = 0.$$

The solution can be found using the software Mathematica [22]. There are two sets of solutions, two of the solutions are purely real, two purely imaginary and each pair has the same absolute value:

$$m_{11} = \pm\sqrt{\frac{\gamma - 4\alpha m_{12}}{\alpha\gamma M}}, \quad m_{12} = \frac{2\alpha - \gamma - 2\sqrt{\alpha(\alpha - \gamma)}}{\gamma},$$

$$m_{22} = M\sqrt{\alpha(\alpha - \gamma)} m_{11},$$

$$m_{11} = \pm\sqrt{\frac{\gamma - 4\alpha m_{12}}{\alpha\gamma M}}, \quad m_{12} = \frac{2\alpha - \gamma + 2\sqrt{\alpha(\alpha - \gamma)}}{\gamma}, \quad (2.49)$$

$$m_{22} = -M\sqrt{\alpha(\alpha - \gamma)} m_{11}.$$

The second set uses these solutions to calculate the other three elements, without imposing the approximation:

$$\alpha m_{13}^2 + \frac{1}{M} m_{23}^2 + \gamma m_{33}^2 + \frac{2 m_{23}}{M} = \frac{\overline{\omega^2}}{\gamma},$$

$$\alpha m_{11} m_{13} + \frac{1}{M} m_{12} m_{23} + \gamma m_{13} m_{33} + \frac{m_{12} - m_{23}}{M} = 0,$$

$$\alpha m_{12} m_{13} + \frac{1}{M} m_{22} m_{23} + \gamma m_{23} m_{33} + \alpha m_{13} + \frac{m_{22}}{M} - \gamma m_{33} = 0.$$

This set of equations can again be solved using Mathematica, but the final form is rather long and would not fit on the page, so we will not be writing it here. All three are approximately constant $m_{13} \approx 0, m_{23} \approx -1, m_{33} \approx \frac{\sqrt{\overline{\omega^2}}}{\gamma}$. Overall, when taking into account that the matrix $\mathbb{M}$ is positive definite, the results are approximately:

$$m_{11} = \sqrt{\frac{\gamma - 4\alpha m_{12}}{\alpha\gamma M}}, \quad m_{12} = \frac{2\alpha - \gamma - 2\sqrt{\alpha(\alpha - \gamma)}}{\gamma}, \quad m_{13} = 0, \quad (2.50a)$$

$$m_{22} = M\sqrt{\alpha(\alpha - \gamma)} m_{11}, \quad m_{23} = -1, \quad m_{33} = \frac{\sqrt{\overline{\omega^2}}}{\gamma}, \quad (2.50b)$$

where we can see that the values m_{13} and m_{23} are in accordance with our approximation.

The Riccati equation can be solved numerically using the programming language Julia, as was said above. Comparing the approximate but analytical solution found through Mathematica with this numerical solution for some given parameters $\alpha, \gamma, \overline{\omega^2}$ and M shows similar results. However, the approximation can be used only for some set of parameters α, γ, M and $\overline{\omega^2}$. In Chapter 3, we will

numerically compare the values calculated in (2.50) with the numerical values. With the solution, we found the dissipation potential, which has the form:

$$\psi = \frac{T}{2}\mathbf{y}^{*T}\mathbb{M}\mathbf{y}^* \approx \frac{T}{2}\mathbf{y}^{*T}\begin{pmatrix} m_{11} & m_{12} & 0 \\ m_{12} & m_{22} & -1 \\ 0 & -1 & \frac{\sqrt{\overline{\omega^2}}}{\gamma} \end{pmatrix}\mathbf{y}^* \tag{2.51}$$

For the final equations, a transition of the Poisson bracket is needed as well. This will be done by the change of variables in Equation (2.24), i.e. starting from this equation, we expect the functions to be $A = A(\overline{Q}, \overline{P}, \overline{s})$, $B = B(\overline{Q}, \overline{P}, \overline{s})$. By chain rule, we have

$$\frac{\delta A}{\delta f} = \frac{\partial A}{\partial y^a}\frac{\delta y^a}{\delta f}$$

Using Equation (2.29) and denoting $\frac{\partial A}{\partial y^a} = A_{y^a}$, we have:

$$\{A, B\}^{(f)} = N! \int ... \int \mathrm{d}Q...\mathrm{d}N f \left[\frac{\partial}{\partial Q}\left(A_{\overline{Q}}\frac{\delta \overline{Q}}{\delta f} + A_{\overline{s}}\frac{\delta \overline{s}}{\delta f} \right)\frac{\partial}{\partial P}\left(B_{\overline{P}}\frac{\delta \overline{P}}{\delta f} \right) - .. \right]$$

Since none of the differentials from Equation (2.29) is dependent on p_i, all the terms with derivatives of the unresolved particles drop out. The final result is

$$\frac{\partial A}{\partial y^a}^{\downarrow} L^{ab}\frac{\partial B}{\partial y^b} = {}^{\downarrow}\{A, B\} = \left(A_{\overline{Q}} - A_{\overline{s}} \right) B_{\overline{P}} - \left(B_{\overline{Q}} - B_{\overline{s}} \right) A_{\overline{P}}. \tag{2.52}$$

We can now, in **step nine** of the procedure, write the evolution equations for $\overline{Q}, \overline{P}$ and $\overline{s}$, using the energy given in Equation (2.36) and the lower Poisson bivector 2.52. The detailed evolution can be also found simply by writing $\mathbf{y}^*(\mathbf{y})$ in Equation (2.45). These two roads lead to the same endpoint (as was shown in Equation (1.20)) and thus we verified the accuracy of our calculations. The evolution equations are:

$$\dot{\overline{Q}} = \frac{\overline{P}}{M} - m_{11}\alpha\overline{Q} - m_{12}\frac{\overline{P}}{M} - m_{13}\gamma\overline{s}, \tag{2.53a}$$

$$\dot{\overline{P}} = \gamma\overline{s} - \alpha\overline{Q} - m_{12}\alpha\overline{Q} - m_{22}\frac{\overline{P}}{M} - m_{23}\gamma\overline{s}, \tag{2.53b}$$

$$\dot{\overline{s}} = -\frac{\overline{P}}{M} - m_{13}\alpha\overline{Q} - m_{23}\frac{\overline{P}}{M} - m_{33}\gamma\overline{s}. \tag{2.53c}$$

When we apply the approximate solution (2.50) on Equation (2.53), we have:

$$\dot{\overline{Q}} = (1 - m_{12})\frac{\overline{P}}{M} - m_{11}\alpha\overline{Q}, \tag{2.54a}$$

$$\dot{\overline{P}} = -(1 + m_{12})\alpha\overline{Q} - m_{22}\frac{\overline{P}}{M} + 2\gamma\overline{s}, \tag{2.54b}$$

$$\dot{\overline{s}} = -\sqrt{\overline{\omega^2}}\overline{s}. \tag{2.54c}$$

Before concluding this chapter, we will study the other choice of variables.

2.2.1 Solution for the Lower Variables (Q,P)

The calculations for the choice (Q, P) are very similar to the calculations done in the previous subsection. Therefore, we can only review the results.

Step one is the same detailed evolution, i.e. the Liouville equation (2.23).

Step two are projections for $\overline{Q}$ and $\overline{P}$ given in the equations (2.27 a,b) respectively and the energy given in Equation (2.26).

Step three gives the distribution function:

$$\tilde{f} = \frac{1}{h^{N+1}} \exp{-\frac{\nu^*}{k_B}} - 1 \exp{-\frac{QQ^*}{k_B}} \exp{-\frac{PP^*}{k_B}} \exp{-\frac{eE^*}{k_B}}, \qquad (2.55)$$

with the normalisation constant, denoting

$$\Sigma_{QP} = \frac{(Q^*)^2}{2\alpha} + \frac{M(P^*)^2}{2},$$

we write the normalisation constant:

$$\nu^*(\mathbf{y}^*) = \frac{\Sigma_{QP}}{E^*} - (N+1)k_B \ln\left(\frac{E^* \hbar}{k_B}\right) - k_B \ln(N!) - k_B +$$

$$+ \frac{k_B}{2} \ln\left(\frac{M}{\alpha}\right) + \frac{k_B}{2} \sum_{i=1}^{N} \ln\left(\frac{m_i N}{\gamma}\right)$$

and the entropy:

$$^\downarrow S(\mathbf{y}) = k_B(N+1) \ln\frac{U}{\hbar} + S_0 \qquad (2.56)$$

where $U = E - \frac{1}{2}\left(\alpha\overline{Q}^2 + \frac{\overline{P}}{M}\right)$ and S_0 is given as

$$S_0 = k_B \left(\frac{1}{2}\left[\ln\left(\frac{M}{\alpha}\right) - \sum_{i=1}^{N} \ln\left(\frac{m_i N}{\gamma}\right)\right] - \ln N! - (N+1)(\ln(N+1) - 1)\right).$$

Step four is the apparent lower-level energy:

$$^\uparrow \overline{E}(f) = \frac{1}{2}\left(\alpha\overline{Q}^2(f) + \frac{\overline{P}^2(f)}{M}\right) + \hbar \exp{\frac{^\downarrow S(\mathbf{y}(f)) - S_0}{k_B(N+1)}}. \qquad (2.57)$$

Step five gives the residuum:

$$R = \frac{f}{k_B}\left[(\mathbf{y}^{*T}, \dot{\mathbf{y}}^{*T})\mathbf{V} - \dot{\mathbf{y}}^{*T}\mathbf{y}(\mathbf{y}^*)\right],$$

$$\mathbf{V}^T = (\frac{\mathbf{P}}{M}, -\alpha\mathbf{Q} - \frac{\gamma}{N}\sum_i (Q - q_i), 0, \mathbf{Q}, \mathbf{P}, e).$$

In **step six**, the Lagrangian starts deviating a bit more from the previous calculations:

$$\mathcal{L} = \frac{1}{2}(\mathbf{y}^{*T}, \dot{\mathbf{y}}^{*T})\begin{pmatrix} \mathbb{A} & \mathbb{B} \\ \mathbb{B}^T & \mathbb{C} \end{pmatrix}\begin{pmatrix} \mathbf{y}^* \\ \dot{\mathbf{y}}^* \end{pmatrix}, \quad \mathbb{A} = \mathbb{A}^T \in \mathbb{R}^{4\times4}, \quad \mathbb{B} \in \mathbb{R}^{4\times4}, \quad \mathbb{C} = \mathbb{C}^T \in \mathbb{R}^{4\times4}. \qquad (2.58)$$

$$\mathbb{A} = \frac{1}{E^*}\begin{pmatrix} \frac{1}{M} & 0 & 0 \\ 0 & \alpha + \gamma & 0 \\ 0 & 0 & 0 \end{pmatrix}, \mathbb{B} = \frac{1}{E^*}\begin{pmatrix} 0 & 1 & -\frac{P^*}{E^*} \\ -1 & 0 & \frac{Q^*}{E^*} \\ 0 & 0 & 0 \end{pmatrix}, \tag{2.59}$$

$$\mathbb{C} = \frac{1}{E^*}\begin{pmatrix} \frac{1}{\alpha} & 0 & -\frac{Q^*}{E^*\alpha} \\ 0 & M & -\frac{MP^*}{E^*} \\ -\frac{Q^*}{E^*\alpha} & -\frac{MP^*}{E^*} & \frac{k_B E^*(N+1)+2\Sigma_{QP}}{(E^*)^2} \end{pmatrix}. \tag{2.60}$$

Step seven is the same as before, but $\mathbb{C}^{-1}$ takes the form:

$$\mathbb{C}^{-1} = E^*\text{diag}\left(\alpha, \quad \frac{1}{M}, \quad 0\right) + \frac{1}{k_B(N+1)}\begin{pmatrix} Q^* \\ P^* \\ E^* \end{pmatrix}\begin{pmatrix} Q^*, & P^*, & E^* \end{pmatrix}. \tag{2.61}$$

Step eight will again require the same approximations as in the previous section (i.e. constant temperature, neglecting higher orders of Q^*, P^* and the near equilibrium ansatz) and the solution of the Riccati equation, which gives a positive definite matrix, is:

$$m_{11} = \sqrt{\frac{\gamma + 4\alpha m_{12}}{\alpha\gamma M}}, \quad m_{12} = \frac{-2\alpha - \gamma + 2\sqrt{\alpha(\alpha + \gamma)}}{\gamma}, \tag{2.62}$$

$$m_{22} = M\sqrt{\alpha(\alpha + \gamma)}m_{11},$$

which is almost the same as in Equation (2.50). The resulting dissipation potential is:

$$\psi = \frac{T}{2}\mathbf{y}^{*T}\begin{pmatrix} \sqrt{\frac{\gamma + 4\alpha m_{12}}{\alpha\gamma M}} & m_{12} \\ m_{12} & M\sqrt{\alpha(\alpha + \gamma)}m_{11} \end{pmatrix}\mathbf{y}^* \tag{2.63}$$

In **Step nine**, the final set of differential equations is:

$$\dot{\overline{Q}} = \frac{\overline{P}}{M} - m_{11}\alpha\overline{Q} - m_{12}\frac{\overline{P}}{M}, \tag{2.64a}$$

$$\dot{\overline{P}} = -\alpha\overline{Q} - m_{12}\alpha\overline{Q} - m_{22}\frac{\overline{P}}{M}. \tag{2.64b}$$

With this choice of variables, there is no longer any dependence on the distribution of the frequencies ω_i. Both solutions suggests, that as a result of the lack of fit, the potential changes into an effective potential and the same happens for the mass, owing to the terms proportional to $\overline{Q}$ and $\overline{P}$.

2.3 Summary

In this chapter, we have applied the methods studied in Chapter 1 on the Kac-Zwanzig model. The Kac-Zwanzig model is a system of N+1 particles, with N of the particles being considered an undistinguishable. Above that the system is connected to a heat bath with constant temperature T, making the system an isothermal one.

In Section 2.1, we applied the Mori-Zwanzig formalism for two choices of projections – first of them is the position and momentum of the distinguished particle (Q,P) and the second choice is (Q,P,s), where $s = \frac{1}{N} \sum_{i=1}^{N} q_i - Q$. We made a detailed derivation of the orthogonal evolution for the choice of resolved variables (Q, P, s). The solution of (Q, P) was straightforward and required no such thing. In the end, we arrived at two sets of equations, each of them having only one equation with memory kernel and a random force. The evolution equations for (Q, P, s) are an original result of this thesis.

Before proceeding to the second method, we reviewed results presented in [16] of a limit as $N \to \infty$ for the projection (Q,P). This led to a set of stochastic differential equations, which resembled the equations for projection (Q, P, s). This resemblence was the motivation for the choice of resolved variables (Q,P,s) in the first place.

In Section 2.2. , we went through the algorithm of the lack-of-fit reduction outlined in the subsection 1.3.2. On the upper level we opted for a description with distribution functions f. The lower variables were the mean values $(\overline{Q}, \overline{P}, \overline{s}, E)$ as well as $(\overline{Q}, \overline{P}, E)$, with energy being a variable in order to introduce temperature to the system. For $(\overline{Q}, \overline{P}, \overline{s})$ we went through all the calculations needed in detail, whereas for $(\overline{Q}, \overline{P})$ only results were given. When solving the Hamilton-Jacobi equation, we set the temperature constant and made a near-equilibrium quadratic ansatz of the dissipation potential. This gave us the Riccati equation and in turn the final evolution equations. In contrast to our theory, the dissipation potential has both reversible and irreversible terms. This suggests an appearance of effective potentials and masses. The calculations done in Section 2.2 with the resulting evolution equations are an original work, which tests the lack-of-fit theory as formulated in [10].

The following section will examine the comparison of the equations we obtained in this chapter with the help of numerical experiments.

3. Comparison through Numerical Experiments

In this last section, we will examine how the theoretical methods correspond to a numerical experiment as well as to each other. In the numerical simulation, we model the stochastic differential equations (2.22) and the ordinary differential equations (2.64) and (2.53). Both simulations are done in the programming language Julia. The ODE integrator is chosen by the programming language itself, as is recommended in the official documentation for the package DifferentialEquation.jl [21]. An argument "alg_hints=[:stiff]" was used to ensure small error in case the problem was stiff. Our stochastic differential equation (SDE) is an Itô problem [23] and therefore the SDE integrator is chosen by recommendation to be SOSRI with an adaptive step [21]. The SOSRI integrator was tested for several decreasingly small step sizes and the results matched the adaptive step. These choices of integrators thus should be sufficient on the studied time scales.

Before the numerical experiments, we will first compare the form of the evolution equations.

3.1 Comparison of the Equations

We will study the comparison of the evolution equations resulting from the Mori-Zwanzig formalism (2.17) and (2.18), with the lower-level evolution equations given by the lack-of-fit reduction (2.64) and (2.53). The lack-of-fit reduction was done in the one-dimensional case and with the harmonic potential, therefore we will impose this on the Mori-Zwanzig equations as well. Furthermore, the comparison can be done only after finding the mean values of the equations with respect to the distributions $\tilde{f}$. For the resolved variables (Q, P), the extremal distribution is a multivariate normal distribution with the means

$$(\mu_Q, \mu_{qi}, \mu_P, \mu_{pi}) = (\overline{Q}, \overline{Q}, \overline{P}, 0)$$

and the covariance matrix

$$\Sigma = \begin{pmatrix} \Sigma_q & 0 \\ 0 & \Sigma_p \end{pmatrix}, \Sigma_q = \frac{1}{\beta} \begin{pmatrix} \frac{1}{\alpha} & \frac{1}{\alpha} & \frac{1}{\alpha} & \dots \\ \frac{1}{\alpha} & \frac{1}{\alpha} + \frac{N}{\gamma} & \frac{1}{\alpha} & \dots \\ \frac{1}{\alpha} & \frac{1}{\alpha} & \frac{1}{\alpha} + \frac{N}{\gamma} & \dots \\ \dots & & & \end{pmatrix}, \Sigma_p = \frac{1}{\beta} \begin{pmatrix} \frac{1}{M} & 0 & 0 & \dots \\ 0 & \frac{1}{m_1} & 0 & 0 & \dots \\ 0 & 0 & \frac{1}{m_2} & 0 & \dots \\ \dots & & & & \end{pmatrix}.$$

For the resolved variables (Q, P, s), the extremal distribution is a multivariate normal distribution with the mean values

$$(\mu_Q, \mu_{qi}, \mu_P, \mu_{pi}) = (\overline{Q}, \overline{Q} + \overline{s}, \overline{P}, 0)$$

and the same covariance matrix Σ.

Both forces F and F_s have a zero mean and when using the harmonic potential, the equations (2.17) and (2.18) are linear in all initial conditions. As a consequence, we have the equations for $(\overline{Q}, \overline{P}, \overline{s})$:

$$\frac{\partial}{\partial t} S^t \overline{Q} = S^t \left(\frac{\overline{P}}{M} \right), \tag{3.1a}$$

$$\frac{\partial}{\partial t} S^t \overline{P} = -S^t(\alpha \overline{Q}) + S^t(\gamma \overline{s}), \tag{3.1b}$$

$$\frac{\partial}{\partial t} S^t \overline{s} = -S^t \frac{\overline{P}}{M} - \int_0^t K_{\mathbf{s}}(u) S^{t-u} \overline{s} du, \tag{3.1c}$$

and also for $(\overline{Q}, \overline{P})$:

$$\frac{\partial}{\partial t} S^t \overline{Q} = S^t \left(\frac{\overline{P}}{M} \right), \tag{3.2a}$$

$$\frac{\partial}{\partial t} S^t \overline{P} = -S^t(\alpha \overline{Q}) - \int_0^t K(u) S^{t-u} \frac{\overline{P}}{M} du. \tag{3.2b}$$

The reversible part of the evolutions is the same as the parts corresponding to the Poisson bracket in equations (2.53) and (2.64). However, the lack-of-fit reduction has additional terms from the dissipation potential. Further analysis requires either closer examination of the dissipation matrices $\mathbb{M}$ or moving to the limit $N \to \infty$, where the equations (2.17) become a system of stochastic differential equations (2.22).

We will first focus more on the lack-of-fit solutions. The solution for resolved variables (Q, P, s) is a matrix exponential of the matrix Sol:

$$\text{Sol} = \begin{pmatrix} -\alpha m_{11} & \frac{1}{M}\left(1 - m_{12}\right) & -m_{13}\gamma \\ -\alpha\left(1 + m_{12}\right) & -\frac{m_{22}}{M} & \left(1 - m_{23}\right)\gamma \\ -m_{13}\alpha & -\frac{1}{M}\left(1 + m_{23}\right) & -m_{33}\gamma \end{pmatrix}.$$

By the Gershgorin circle theorem [24] the eigenvalues are within circles in the imaginary plane:

$$|\lambda + \alpha m_{11}| \le \alpha\left(|m_{13}| + |1 + m_{12}|\right), \tag{3.3a}$$

$$|\lambda + \alpha m_{11}| \le \frac{1}{M}|1 - m_{12}| + \gamma|m_{13}|, \tag{3.3b}$$

$$\left|\lambda + \frac{m_{22}}{M}\right| \le \frac{1}{M}\left(|1 - m_{12}| + |1 + m_{23}|\right), \tag{3.3c}$$

$$\left|\lambda + \frac{m_{22}}{M}\right| \le \alpha\left|1 + m_{12}\right| + \gamma\left|1 - m_{23}\right|, \tag{3.3d}$$

$$|\lambda + m_{33}\gamma| \le \gamma\left(|1 - m_{23}| + |m_{13}|\right), \tag{3.3e}$$

$$|\lambda + m_{33}\gamma| \le \alpha|m_{13}| + \frac{1}{M}|1 + m_{23}|. \tag{3.3f}$$

We may expect that for large $m_{33}\gamma$ (i.e. large second moment of the distribution of the frequencies) the circle defined in (3.3e,f) is disjoint from the other two. We

may also expect one of the eigenvalues to be $\lambda = -m_{33}\gamma \approx -\overline{\omega^2}$, which would give us a time scale of damping. Let us examine the numerical solutions for different parameters, which will give us a better notion of the results and how they align with our approximate solutions (2.50). In each of the figures 3.1-3.3, we show nine contour plots: three of them (displayed in the first column) correspond to the numerical values of m_{11}, m_{12} and m_{22}, another three (second column) show the difference $R_{ij}, i, j \in \{1, 2\}$ between these numerical values and the corresponding approximate solutions (2.50) and the last three show the difference from the approximate solution for the last three matrix elements $R_{13} = m_{13}$, $R_{23} = m_{23} + 1$ and $R_{33} = m_{33} - \frac{\overline{\omega^2}}{\gamma}$. Note that in the previous section R_{13} and R_{23} were denoted $\tilde{m}_{13}, \tilde{m}_{23}$.

With larger $\overline{\omega^2}$ (as well as with larger M) the precision of the approximation of the elements m_{13}, m_{23} and m_{33} grows. The rift in the values of R_{12}, R_{11} and R_{22} is caused by the fact that for certain values our approximation is no longer sufficient and gives purely imaginary results. Thus, we search for an absolute value under the square root, even though perhaps different root from 2.49 would give better results.

Now we can compare the results with the equation (3.1). The first equation (3.1a) is the same as in the lack-of-fit evolution if m_{1i} were 0, $\forall i$. In the figures we see that with larger M and $\overline{\omega^2}$, m_{13} is almost zero. Large M will also decrease the influence of the element m_{12}. The term m_{11} would then require larger values of γ so that we may choose smaller α. The equation for s in this case would be almost precisely corresponding to the evolution equation (2.54c) and therefore would be different from the equation (3.1c). This would disrupt the similarities between the solutions from the Mori-Zwanzig formalism and the lack of fit reduction. As such, the lack-of-fit reduction has more prominent damping terms.

The comparison of the equations for the variables (Q, P) is more straight forward, but similar in nature. In the solution of $\mathbb{M}$, the value of m_{22}, which we expect to stand in place of the memory kernel, is directly proportional to m_{11}, which is zero in the Mori-Zwanzig equations.

The comparison of the SDE (2.22) and the two sets of ODEs from the lack-of-fit procedure (2.53), (2.64) is troublesome. To reach the equations (2.22), we needed to have the frequencies ω_i from the Cauchy distribution. However, the second moment of the Cauchy distribution, necessary for the calculations of $\mathbb{M}$, is infinit. Nevertheless, we will compare the equations numerically and opt for a large value of the second moment.

3.2 Numerical comparison of lack-of-fit and SDE

In the first comparison, we will fix $\alpha = 10$, $\beta = 300$, $\overline{\omega^2} = 10^8$, initial conditions $(Q_0, P_0, s_0) = (1, 0, 0)$ and observe the behaviour of the solutions for different M and γ. The comparison starts with larger set of values for M within each figure and different choice of γ for the different figures, thus placing focus on the dependence on M. The results are ploted in Figures 3.4, 3.5 and 3.6
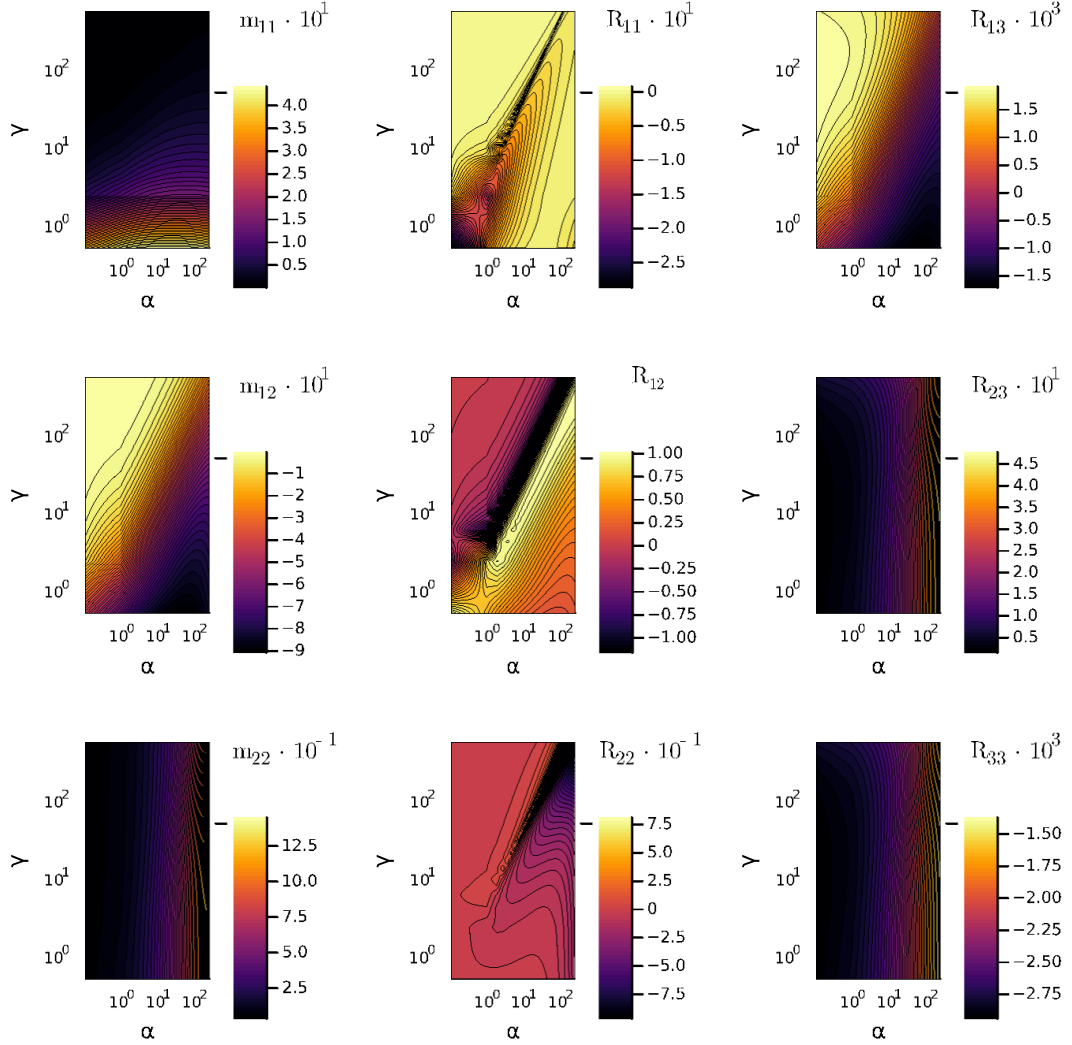
Figure 3.1: Numerical values of the elements of the dissipation matrix $\mathbb{M}$ and the differences R_{ij} from the calculated approximate values (2.50).We fixed $M = 50$, $\overline{\omega^2} = 10^2$, $\alpha \in (0.1, 250)$ and $\gamma \in (0.5, 550)$. The approximate values of the elements (m_{13}, m_{23}, m_{33}) are given as $(0, -1, \frac{\overline{\omega^2}}{\gamma})$ and only the difference R_{ij} from the numerical value is plotted. The values of the matrix elements displayed on the colorbars are scaled as is stated in above the colour bars.
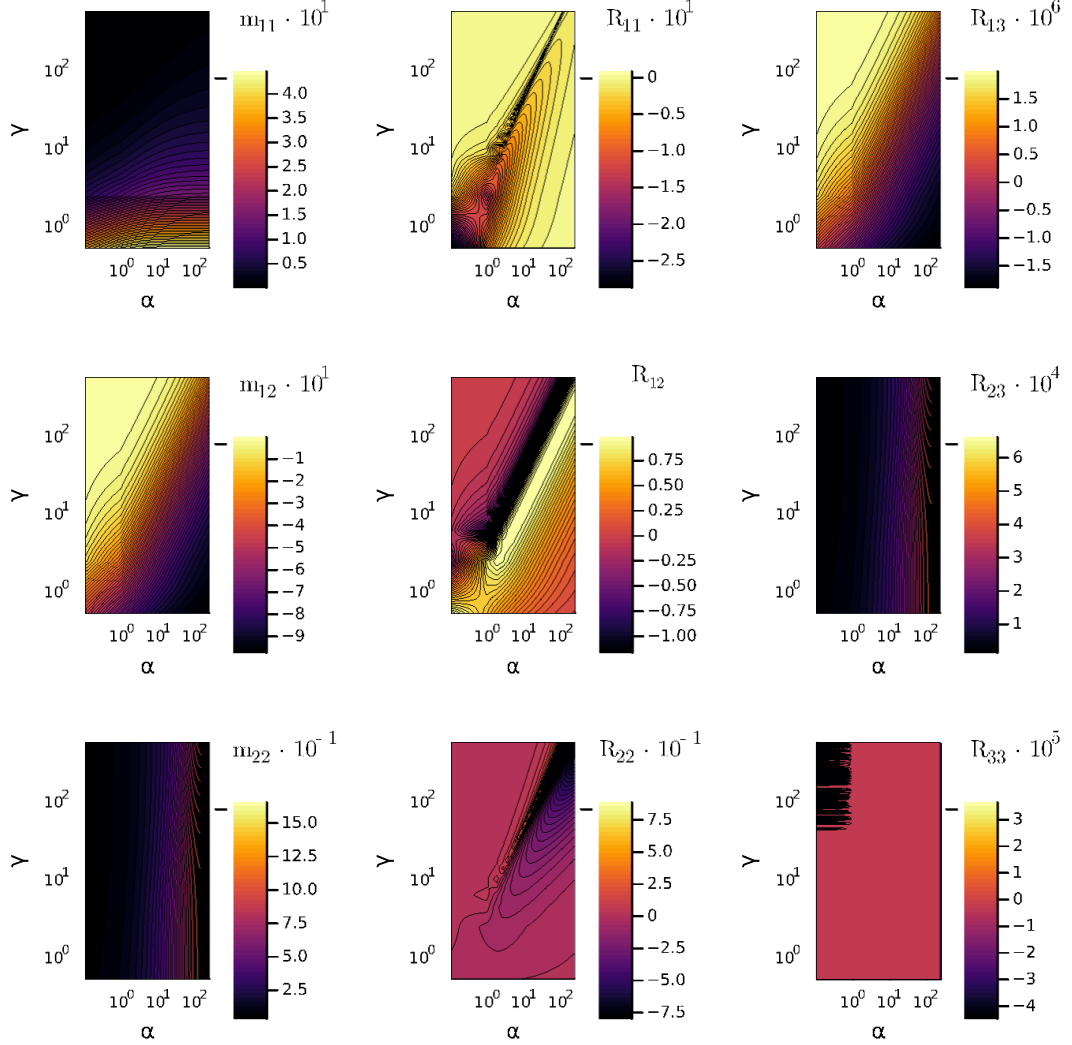
Figure 3.2: Numerical values of the elements of the dissipation matrix $\mathbb{M}$ and the differences R_{ij} from the calculated approximate values (2.50).We fixed $M = 50$, $\overline{\omega^2} = 10^8$, $\alpha \in (0.1, 250)$ and $\gamma \in (0.5, 550)$. The approximate values of the elements (m_{13}, m_{23}, m_{33}) are given as $(0, -1, \frac{\overline{\omega^2}}{\gamma})$ and only the difference R_{ij} from the numerical value is plotted. The values of the matrix elements displayed on the colorbars are scaled as is stated in above the colour bars.
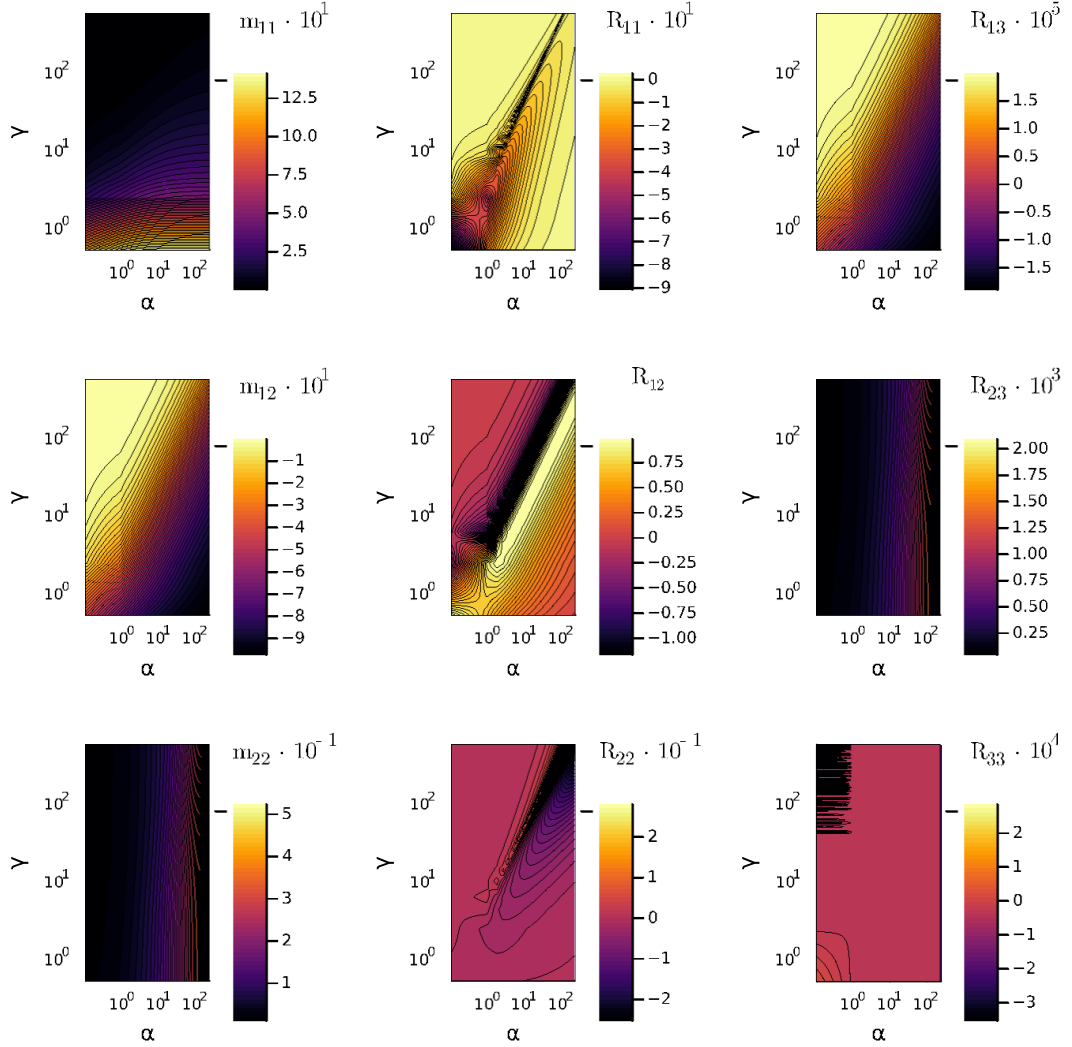
Figure 3.3: Numerical values of the elements of the dissipation matrix $\mathbb{M}$ and the differences R_{ij} from the calculated approximate values (2.50).We fixed $M = 5$, $\overline{\omega^2} = 10^8$, $\alpha \in (0.1, 250)$ and $\gamma \in (0.5, 550)$. The approximate values of the elements (m_{13}, m_{23}, m_{33}) are given as $(0, -1, \frac{\overline{\omega^2}}{\gamma})$ and only the difference R_{ij} from the numerical value is plotted. The values of the matrix elements displayed on the colorbars are scaled as is stated in above the colour bars.
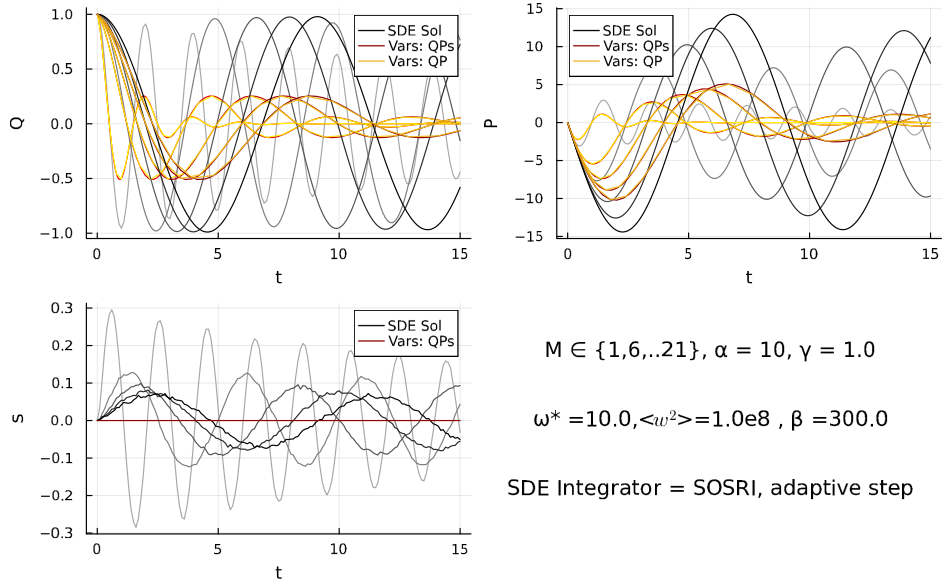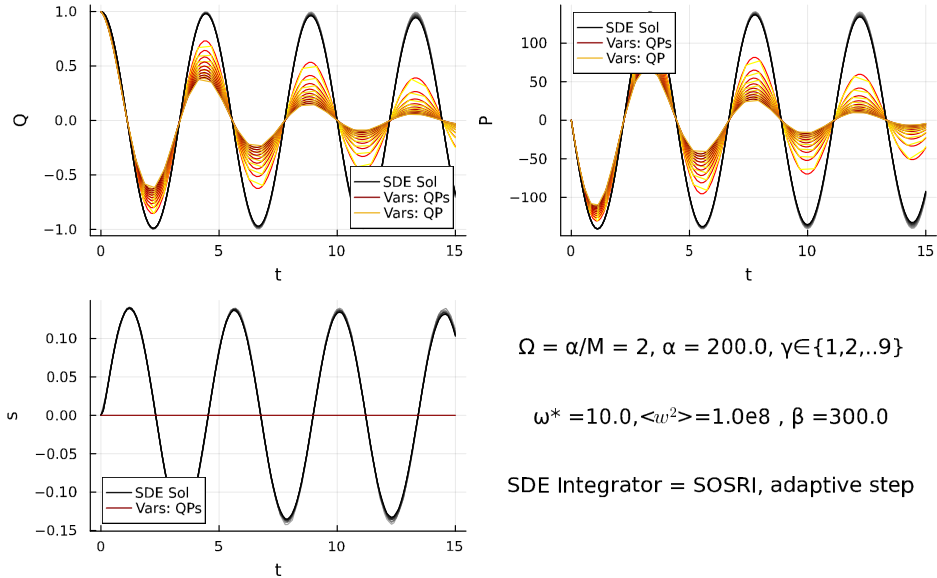
Figure 3.4: The time evolution of variables Q, P and s. Yellow and red lines are indistinguishable and correspond to the lack-of-fit reduction, where s is the mean distance of the cloud from the distinguished particle. Grayscale lines correspond to the limit SDE, where s was variable, which replaced an exponential memory kernel. Different hues from lighter to darker correspond to $M \in \{1, 6, 11, 16, 21\}$. The SDE is a mean value of 400 runs.
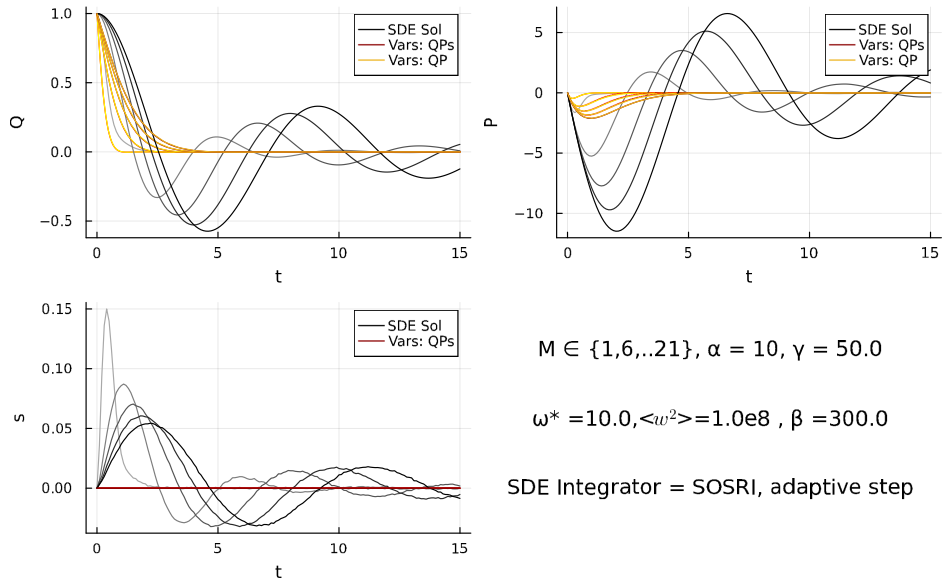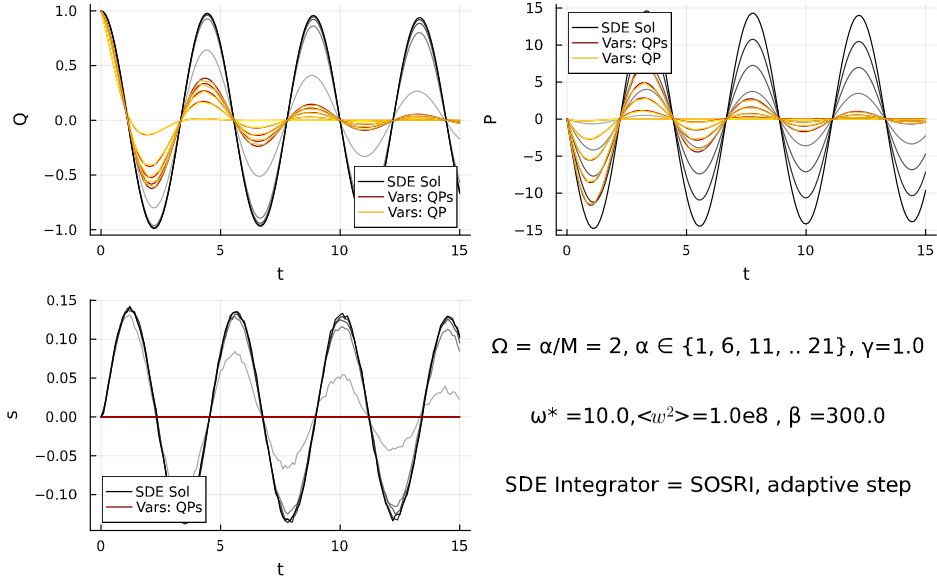

Figure 3.5: The time evolution of variables Q, P and s. Yellow and red lines are indistinguishable and correspond to the lack-of-fit reduction, where s is the mean distance of the cloud from the distinguished particle. Grayscale lines correspond to the limit SDE, where s was variable, which replaced an exponential memory kernel. Different hues from lighter to darker correspond to $M \in \{1, 6, 11, 16, 21\}$. The SDE is a mean value of 400 runs.
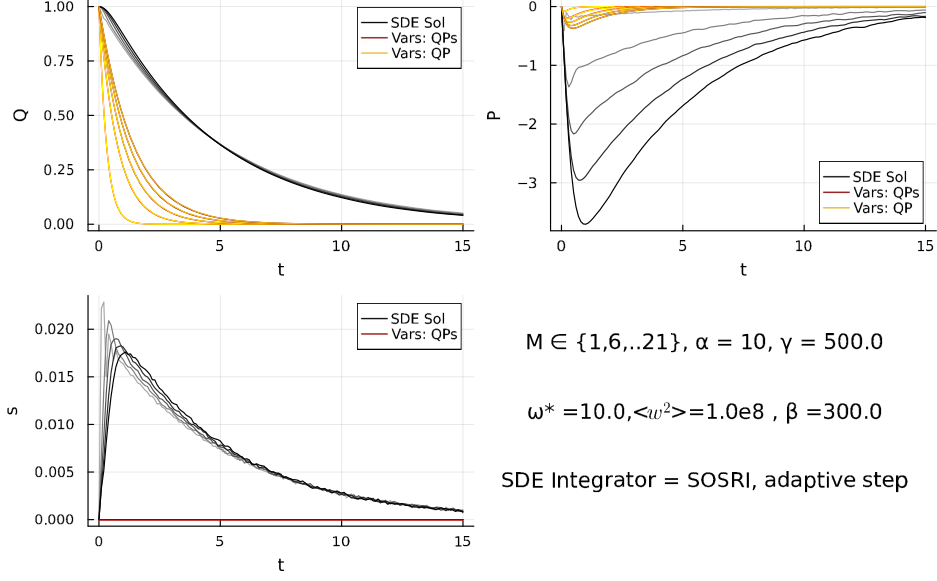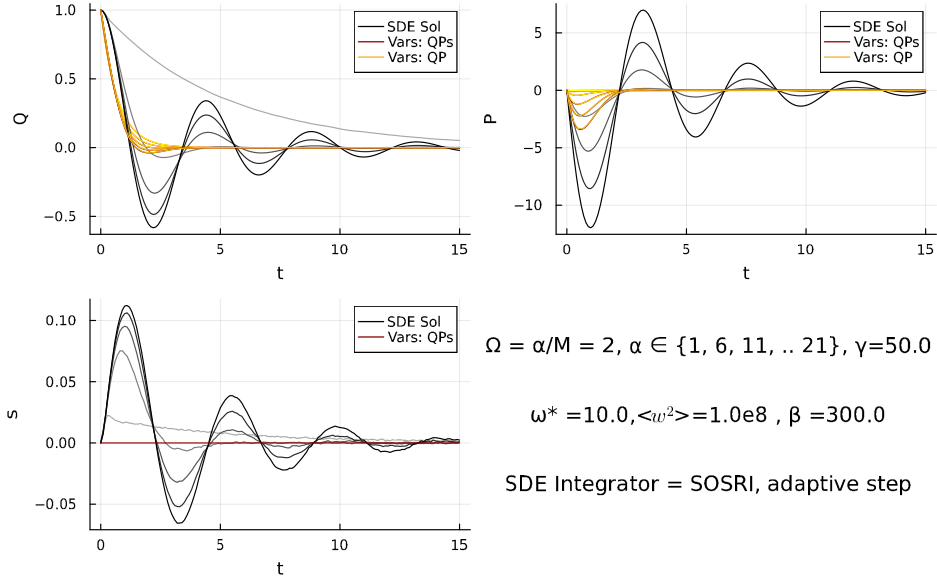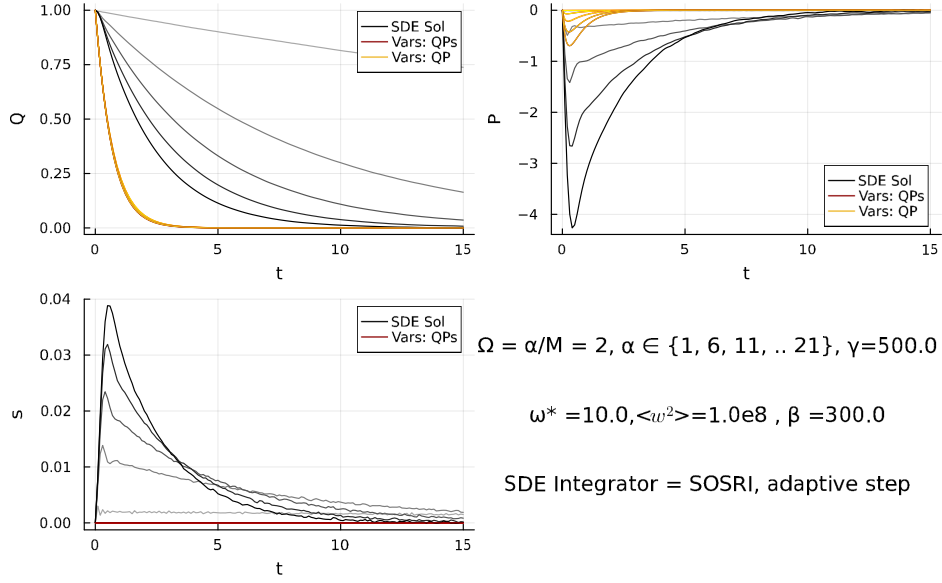
Figure 3.6: The time evolution of variables Q, P and s. Yellow and red lines are indistinguishable and correspond to the lack-of-fit reduction, where s is the mean distance of the cloud from the distinguished particle. Grayscale lines correspond to the limit SDE, where s was variable, which replaced an exponential memory kernel. Different hues from lighter to darker correspond to $M \in \{1, 6, 11, 16, 21\}$. The SDE is a mean value of 800 runs.

In these three figures, darker hues correspond to larger M, where M has five values, $M \in \{1, 6, 11, 16, 21\}$. Additionally, each figure has different γ from the set of values $\{1, 50, 500\}$, thus studying two degrees of freedom in the parameters.

In Figure 3.4, the spring constant γ is equal to 1. For all masses M, the lack-of-fit solution dampens faster. Above that, with the initial condition $s_0 = 0$, the s has negligible value compared to the evolution of s from the SDE. The damping changes only slightly in the chosen range of values, only the lowest mass $M = 1$ shows significant difference on the chosen time interval. More significant change happens with the oscillation frequency of both evolution. In the lightest hues, we may also observe that the frequency of all the evolution coincides. In the evolution of s for larger values of M, the stochasticity is more noticeable.

In Figure 3.5, we see that with $\gamma = 50$ the damping is more pronounced. The lack-of-fit evolutions become overdamped, i.e. they no longer have oscillations. The stochastic evolution is still underdamped for all M except for $M = 1$.

In Figure 3.6, the parameter was fixed to the value $\gamma = 500$ and all the evolutions are overdamped. The speed of the damping differs dramatically between the ordinary and stochastic equations even at time zero. The SDE has visibly zero derivative of Q. On the other hand, the lack-of-fit equations, owing to the term $-\alpha m_{11} Q$, have negative derivative and the damping is sped up. In this figure it is especially clear. The source of the difference is likely linked to the fact that the lack-of-fit reduction assumes free initial conditions and long time limit $t \to \infty$. Future work should take this into account, building on the work done in [25, 26, 27].

By comparing the figures 3.4 - 3.6, we observe several effects. First is that

with growing γ, the evolution is more damped for all methods. Furthermore, with growing M both the oscillation and the damping slow down. Above that, we might link the change of M mainly to the change of timescale of these phenomena. We may expect the oscillation frequency to be connected to the natural frequency $\Omega \equiv \frac{\alpha}{M}$. Another observation is that since $s = 0$ for all times, the evolutions of lack-of-fit solutions for (Q, P, s) and (Q, P) are almost identical in the variables Q and P in all figures.

From these observations we are lead to another set of parameter choices: changing values of γ and α for a fixed Ω (Figure 3.7, 3.8 and 3.12) and changes in the initial condition of s (Figure 3.13).
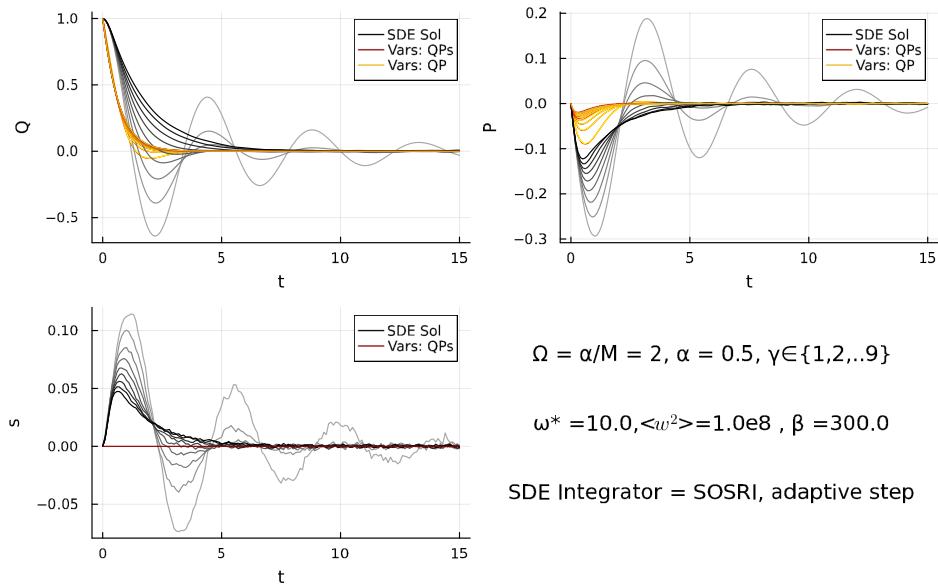
Figure 3.7: The time evolution of variables Q, P and s. Yellow and red lines are indistinguishable and correspond to the lack-of-fit reduction, where s is the mean distance of undistinguished particles from the distinguished one. Grayscale lines correspond to the limit SDE, where s was variable, which replaced an exponential memory kernel. Different hues from lighter to darker correspond to $\gamma \in \{i\}_{i=1}^{9}$ and the SDE is a mean value of 800 runs.

In Figure 3.7, all evolutions are around the transition between an underdamped and overdamped system. Figure 3.8 visibly shows, that γ only changes the speed of damping and has no effect on the frequency of oscillations. In the following figure, 3.9, we observe that the damping of lack-of-fit evolution grows faster with increasing γ than for the SDE. The SDE in the chosen time frame is almost undamped for all γ.

In Figure 3.10, α is taken from the set of values $\{1, 6, 11, 16, 21\}$ and since $\Omega = 2$ the value of mass M is also changed for each evolution, given by α as $\{0.5, 3, 5.5, 8, 10.5\}$. An apt comparison is between the pairs of figures 3.4, 3.10 and 3.6 3.12. Let us note that the natural frequencies Ω in the figures 3.4-3.6 were approximately $\{10, 1.7, 0.9, 0.6, 0.5\}$. In Figure 3.4, we only saw the change of frequency for any larger M than 1 and even for $M = 1$ only the SDE had faster decline. On the other hand, the damping of the lack-of-fit solution in Figure 3.10 of Q is visibly decreasing with larger α and the grayscale SDE damps only for
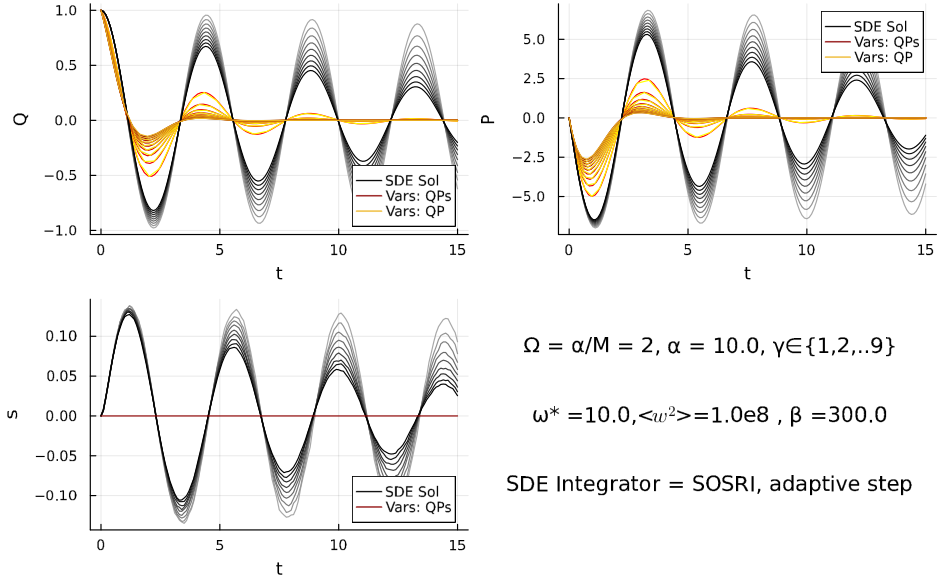
Figure 3.8: The time evolution of variables Q, P and s. Yellow and red lines are indistinguishable and correspond to the lack-of-fit reduction, where s is the mean distance of undistinguished particles from the distinguished one. Grayscale lines correspond to the limit SDE, where s was variable, which replaced an exponential memory kernel. Different hues from lighter to darker correspond to $\gamma \in \{i\}_{i=1}^{9}$ and the SDE is a mean value of 800 runs.

Figure 3.9: The time evolution of variables Q, P and s. Yellow and red lines are indistinguishable and correspond to the lack-of-fit reduction, where s is the mean distance of undistinguished particles from the distinguished one. Grayscale lines correspond to the limit SDE, where s was variable, which replaced an exponential memory kernel. Different hues from lighter to darker correspond to $\gamma \in \{i\}_{i=1}^{9}$ and the SDE is a mean value of 1000 runs.

Figure 3.10: The time evolution of variables Q, P and s. Yellow and red lines are indistinguishable and correspond to the lack-of-fit reduction, where s is the mean distance of undistinguished particles from the distinguished one. Grayscale lines correspond to the limit SDE, where s was variable, which replaced an exponential memory kernel. Different hues from lighter to darker correspond to $\alpha \in \{1, 6, 11, 16, 21\}$ and the SDE is a mean value of 800 runs.

Figure 3.11: The time evolution of variables Q, P and s. Yellow and red lines are indistinguishable and correspond to the lack-of-fit reduction, where s is the mean distance of undistinguished particles from the distinguished one. Grayscale lines correspond to the limit SDE, where s was variable, which replaced an exponential memory kernel. Different hues from lighter to darker correspond to $\alpha \in \{1, 6, 11, 16, 21\}$ and the SDE is a mean value of 800 runs.

Figure 3.12: The time evolution of variables Q, P and s. Yellow and red lines are indistinguishable and correspond to the lack-of-fit reduction, where s is the mean distance of undistinguished particles from the distinguished one. Grayscale lines correspond to the limit SDE, where s was variable, which replaced an exponential memory kernel. Different hues from lighter to darker correspond to $\alpha \in \{1, 6, 11, 16, 21\}$ and the SDE is a mean value of 800 runs.
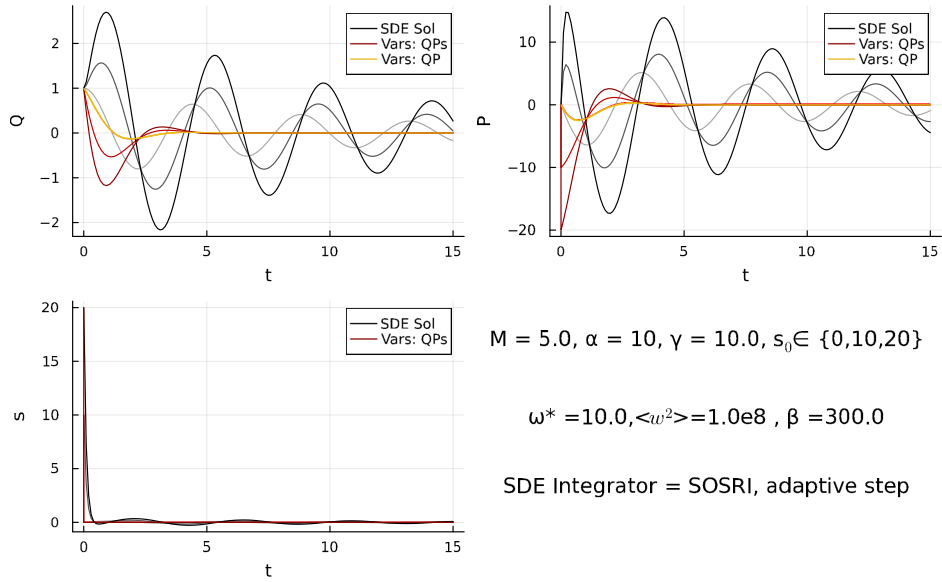
Figure 3.13: The evolution of position Q and momentum P the distinguished particle and the evolution of s. Yellow and red lines correspond to the lack-of-fit reduction with resolved variables (Q, P) and (Q, P, s) respectively. Here s is the mean distance of undistinguished particles from the distinguished one. Grey and black lines correspond to the limit SDE, where s was variable, which replaced an exponential memory kernel. Different hues from lighter to darker correspond to the initial condition of $s \in \{0, 10, 20\}$ and the SDE is a mean value of 800 runs.

the smallest $M = 0.5, \alpha = 1$. In figures 3.6 and 3.12, we see this more clearly – change of M for fixed α changes the damping of the lack-of-fit solution and does not change the SDE, whereas change in both M and α for fixed Ω changes the SDE damping but does not alter the lack-of-fit evolution.

Last figure 3.14 shows the independence of all the evolutions on the second moment $\overline{\omega^2}$.
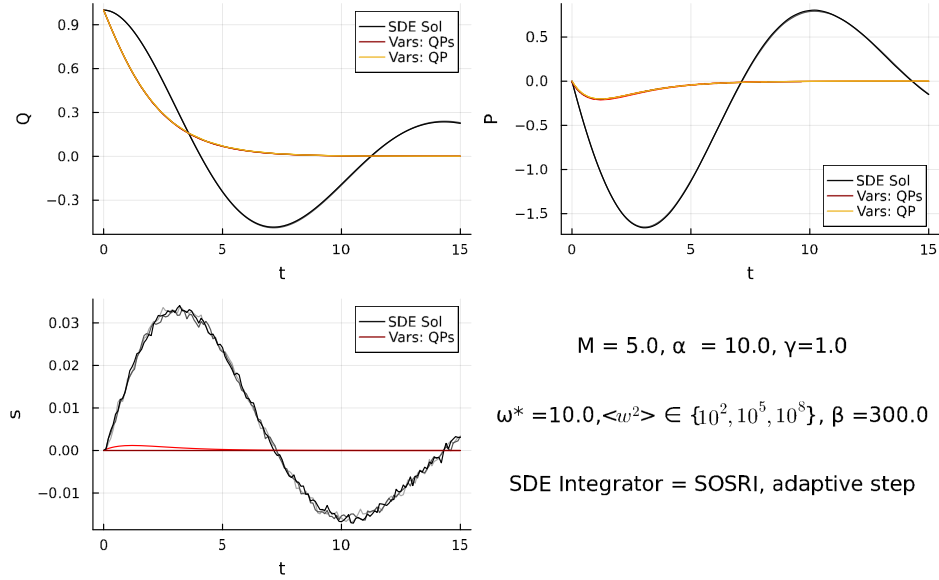
Figure 3.14: The evolution of position Q and momentum P the distinguished particle and the evolution of s. Yellow and red lines correspond to the lack-of-fit reduction with resolved variables (Q, P) and (Q, P, s) respectively. Here s is the mean distance of undistinguished particles from the distinguished one. Grey and black lines correspond to the limit SDE, where s was variable, which replaced an exponential memory kernel. Different hues from lighter to darker correspond to $\overline{\omega^2} \in \left\{10^2, 10^5, 10^8\right\}$ and the SDE is a mean value of 400 runs.

From these figures we are lead to several key results. First is that for both equations we have the same natural frequency, owing to the harmonic potential. Damping in both cases is influenced by the spring constant γ. There are no other significant similarities between the evolutions. The most important result is that the choice of additional variable s in the system does not correspond to the variable created from the exponential memory kernel in the SDE. Another important result is that the lack-of-fit reduction has faster damping for any choice of variables and the results are almost independent on the parameter $\overline{\omega^2}$ as long as its large. No further relation on $\overline{\omega^2}$ is not studied since the comparison between the SDE and the lack-of-fit evolutions loses any meaning for small $\overline{\omega^2}$. This could have been concluded already from the Gershgorin circles written in the equation (3.3e, f). The origin of one of the circles is precisely this second moment and when it is large, it is disjoint from all the other circles. This, yet again, clearly shows the differences between the results of the lack-of-fit reduction and the Mori-Zwanzig formalism.

3.3 Summary

In the last Chapter, we focused on the comparison of the results given in Chapter 2. In Section 3.1, we compared the forms of the evolution equations resulting from the two methods applied in Chapter 2. This involved finding the mean value of the Mori-Zwanzig equations with respect to the maximising distribution function $\tilde{f}$. Afterwards, we took a closer look at the solution of the Riccati equation for lower variables (Q, P, s), using numerical solution. The solutions were plotted as contour plots with axes α and γ, for two different values of $M \in \{5, 50\}$ and two different values of the second moment of the distribution of the frequencies ω_i, $\overline{\omega^2} \in \{10^2, 10^8\}$. We observed that with growing M and $\overline{\omega^2}$ the values of $m_{13}, m_{23}, \gamma m_{33}$ go to $0, -1$ and $\overline{\omega^2}$ respectively. This leads to an important incompatibility of the lack-of-fit solution with the solution given by the Mori-Zwanzig formalism. Similar incompatibility appears for the choice of resolved variables (Q,P).

In Section 3.2, we approached the comparison from the perspective of a numerical experiment. The evolution from the lack-of-fit equations were compared to the evolution given by the stochastic differential equations, which resulted from the limit of $N \to \infty$ in Section 1.2.2. The simulations were done for several different sets of parameters. We discovered that the difference between lack-of-fit evolutions for the two choices of resolved variables (Q,P) and (Q,P,s) was negligible for large values of $\overline{\omega^2}$ and initial conditions s_0 near zero. Above that, in Chapter 2 we noted that the choice of variables (Q, P, s) was done based on the stochastic equation, but in the simulations we observed that s in each of these equations behaves rather differently. Overall, we yet again conclude that the two descriptions do not match up.

Conclusion

In the first chapter, we introduced two methods for dimensional reduction, which lead to the appearance of dissipative terms in the evolution. Each of the methods has its own set of problems. The main problem of the Mori-Zwanzig formalism is that the final equations are in an integro-differential form. Without further simplification, the integro-differential form is hard to analyse both analytically and numerically. Even within this thesis this leads to the inability to thoroughly compare the two choices of resolved variables. The lack-of-fit reduction, on the other hand, gives the evolution as a closed set of ordinary differential equations. However, in the procedure we require the solution of the Hamilton-Jacobi equation, which is a partial differential equation. Furthermore, the resulting dissipation potential is (by construction) a function of only the conjugated variables $\mathbf{y}^*$. In comparison, within the GENERIC formalism the dependence of the dissipation potential on the lower variables $\mathbf{y}$ is not only possible, but also quite common – especially when it comes to temperature. Above that, the generalisation from the original work [9] required few steps (such as constriction only on linear projections, using the entropy norm and using the apparent-upper energy) to reach the final equations in GENERIC form. These steps are introduced as postulates, motivated mainly by the requirement of the specific form of equations and as such need a better explanation or generalisation in the future.

In Chapter 2, we apply the methods on the Kac-Zwanzig model. The results of the two methods significantly differ in form. As a consequence, there are several conclusions to be drawn, most of which would require further work to be done for a more robust interpretation of these results. When it comes to the Mori-Zwanzig formalism, we mainly reviewed work, which was already done [3, 16, 17, 18]. To our knowledge, the choice of variables $(\mathbf{Q}, \mathbf{P}, \mathbf{s})$, with $\mathbf{s}$ being the mean distance of the heat bath particles from the distinguished particle, have not been done before and is our original contribution. The addition of the third variable hoped to give another degree of freedom and thus lead to a more detailed description, ideally one that in a limit would give a system of ODEs. Contrary to this ambition, we arrive yet again at a system of integro-differential equations and within this work we did not succeed at finding the desired limiting ODEs. There are still techniques we have not deployed. The probability distribution of the implicit frequencies ω_{Ql} can be further studied as well as the case for deterministic distribution of ω_i (e.g. $\omega_i = i$, which for the resolved variables $(\mathbf{Q}, \mathbf{P})$ leads to a Fourier series [20]). Theories of random matrices might also be helpful, to better understand the problem and mean values with respect to the distribution of ω_i could have been found. Such closer inspection of the behaviour of $\mathbf{s}$ in the Mori-Zwanzig theory would then be helpful in the comparison to the results of the lack-of-fit reduction.

The main focus of the thesis was on the lack-of-fit reduction and its applicability. Here it is necessary to conclude that in the current form, the theory has many weak points. Some of them were mentioned when summarising the theory, other arose throughout the calculations. We limited the calculations only to the one dimensional case and the harmonic potential. In addition, the Hamilton-Jacobi equation was only solved for another set of approximations. From the

numerical results, we expect that some approximation to be too strong because of the speed of the damping. The sources of the damping are thought to be the free initial conditions, long time limit $t \to \infty$ the near-equilibrium ansatz (giving us the Riccati equation) and the time-scale separation (placing $\frac{\partial \psi}{\partial t} = 0$). Future work should take this into account and may refer to [25, 26, 27], where similar issues are discussed. A different approach to the solution of the Hamilton-Jacobi equation would be using NeuralODEs [28, 29], which is a type of deep neural networks. This would simplify the solution of the most troublesome element of the procedure.

In the third chapter, we made a numerical comparison of the final evolution equations. The results are compared only on the lower level of description, i.e. the comparison is done between the limit $N \to \infty$ of the results given by the Mori-Zwanzig formalism and the two sets of ODEs given by the lack-of-fit reduction. The lack-of-fit evolutions are almost identical for any choice of parameters α, M, γ and $\overline{\omega^2}$. On the other hand, the two methods have a very low correspondence for most chosen values. Since the numerical simulation was conducted only on the lower level of description, a simulation which would reliably compare the results of detailed evolution to the resolved evolution would be desirable.

Bibliography

[1] Robert Zwanzig. Memory effects in irreversible thermodynamics. *Phys. Rev.*, 124:983–992, Nov 1961.

[2] Hazime Mori. Transport, collective motion, and Brownian motion. *Progress of Theoretical Physics*, 33(3):423–455, 03 1965.

[3] Freek Witteveen. The Mori-Zwanzig formalism and stochastic modelling of multiscale dynamical systems. Master's thesis, University of Amsterdam, 2016.

[4] Hermann Grabert. *Projection Operator Techniques in Nonequilibrium Statistical Mechanics*. Springer Berlin, Heidelberg, 1982.

[5] S. Chaturvedi and F. Shibata. Time-convolutionless projection operator formalism for elimination of fast variables. applications to Brownian motion. *Zeitschrift für Physik B Condensed Matter*, 35(3):297–308, 1979.

[6] Alexandre J. Chorin, Ole H. Hald, and Raz Kupferman. Optimal prediction and the Mori-Zwanzig representation of irreversible processes. *Proceedings of the National Academy of Sciences (PNAS)*, 2000.

[7] Michal Pavelka, Václav Klika, and Miroslav Grmela. *Multiscale Thermo-Dynamics: Introduction to GENERIC*. De Gruyter, 2018.

[8] Bruce Turkington. An optimization principle for deriving nonequilibrium statistical models of Hamiltonian dynamics. *Journal of Statistical Physics*, 152(3):569–597, 2013.

[9] Jonathan Maack and Bruce Turkington. Reduced models of point vortex systems. *Entropy*, 20(12), 2018.

[10] Michal Pavelka, Václav Klika, and Miroslav Grmela. Generalization of the dynamical lack-of-fit reduction from GENERIC to GENERIC. *Journal of Statistical Physics*, 181, 10 2020.

[11] I. M. Gelfand and S. V. Fomin. *Calculus of variations*. Selected Russian publications in the mathematical sciences. Prentice-Hall, Englewood Cliffs, N.J., rev. english ed. translated and edited by richard a. silverman edition, 1964.

[12] Vladimír Kučera. A review of the matrix Riccati equation. *Kybernetika*, 09(1):(42)–61, 1973.

[13] George W. Ford, Mark Kac, and Péter Mazur. Statistical mechanics of assemblies of coupled oscillators. *Journal of Mathematical Physics*, 6:504–515, 1965.

[14] F. Slanina. *Essentials of Econophysics Modelling*. Titolo collana. OUP Oxford, 2013.

[15] P. a kol Čihák. *Matematická analýza pro fyziky*, volume V. Matfyzpress, 2001.

[16] Gil Ariel and Eric Vanden-Eijnden. Testing transition state theory on Kac-Zwanzig model. *Journal of Statistical Physics*, 126:43–73, 2007.

[17] Gil Ariel and Eric Vanden-Eijnden. A strong limit theorem in the Kac–Zwanzig model. *Nonlinearity*, 22(1):145, dec 2008.

[18] Raz Kupferman, Andrew Stuart, J. Terry, and Paul Tupper. Long-term behavior of large mechanical systems with random initial data. *Stochastics and Dynamics*, 02, 11 2011.

[19] R. Kupferman and A.M. Stuart. Fitting SDE models to nonlinear Kac–Zwanzig heat bath models. *Physica D: Nonlinear Phenomena*, 199(3):279–316, 2004.

[20] A. M. Stuart and J. O. Warren. Analysis and experiments for a computational model of a heat bath. *Journal of Statistical Physics*, 97(3):687–723, 1999.

[21] Jeff Bezanson, Alan Edelman, Stefan Karpinski, and Viral B Shah. Julia: A fresh approach to numerical computing. *SIAM Review*, 59(1):65–98, 2017.

[22] Wolfram Research, Inc. Mathematica, Version 12.0. Champaign, IL, 2019.

[23] C.W. Gardiner. *Handbook of Stochastic Methods for Physics, Chemistry, and the Natural Sciences*. Springer complexity. Springer, 2004.

[24] S. A. Gershgorin. Über die Abgrenzung der Eigenwerte einer Matrix. *Bull. Acad. Sci. URSS*, 1931(6):749–754, 1931.

[25] Bruce Turkington, Qian-Yong Chen, and Simon Thalabard. Coarse-graining two-dimensional turbulence via dynamical optimization. *Nonlinearity*, 29(10):2961–2989, aug 2016.

[26] Richard Kleeman and Bruce E. Turkington. A nonequilibrium statistical model of spectrally truncated Burgers-Hopf dynamics. *Communications on Pure and Applied Mathematics*, 67(12):1905–1946, 2014.

[27] Simon Thalabard and Bruce Turkington. Optimal response to non-equilibrium disturbances under truncated Burgers–Hopf dynamics. *Journal of Physics A: Mathematical and Theoretical*, 50(17):175502, mar 2017.

[28] Ricky T. Q. Chen, Yulia Rubanova, Jesse Bettencourt, and David Duvenaud. Neural ordinary differential equations, 2019.

[29] Martin Šípka, Johannes C. B. Dietschreit, Lukáš Grajciar, and Rafael Gómez-Bombarelli. Differentiable simulations for enhanced sampling of rare events, 2023.

List of Figures